1966

Six and seven pion annihilation modes of 2.7 BeV/c antiprotons on protons

Daryl Eugene Bohning
Iowa State University

SIX AND SEVEN PION ANNIHILATION MODES OF 2.7 BEV/C ANITPROTONS ON PROTONS

by

Daryl Eugene Bohning

A Dissertation Submitted to the
Graduate Faculty in Partial Fulfillment of
The Requirements for the Degree of
DOCTOR OF PHILOSOPHY

Major Subject: Physics

Approved:

Signature was redacted for privacy.

In Charge of Major Work

Signature was redacted for privacy.

Head of Major Department

Signature was redacted for privacy.

Dean of Graduate College

Iowa State University
Of Science and Technology
Ames, Iowa

1966

TABLE OF CONTENTS

I. INTRODUCTION

A. Experiment

The experiment upon which this work is based was performed at Brookhaven National Laboratory in September of 1964 in an effort to add to the knowledge of antiproton-proton interactions. The experiment made use of the 33 BeV Alternating Gradient Synchrotron (AGS) and its supporting facilities, including the 20" Shutt Bubble Chamber. Approximately 90,000 pictures were taken, the resulting film being shared equally between Iowa State University and the University of Colorado as a collaboration between the two.

B. Accelerator

The AGS at Brookhaven is, at present, the largest accelerator in the world, capable of accelerating protons to energies close to 33 BeV. As its name implies, it is a synchrotron, using a changing magnetic field to make possible the containment of the accelerating beam at a fixed radius in its evacuated doughnut-like ring. The designation "alternating gradient" refers to the type of focusing used to keep the particles within the accelerator localized. A series of quadrupole magnets about the ring of the AGS alternately strongly focus the beam horizontally and then vertically by varying and reversing the magnetic field gradient. In this way an overall strongly focused beam is achieved, resulting in low beam attenuation.

To produce the desired particles for the study of different reactions, the circulating proton beam in the synchrotron is made to impinge on targets

of various materials. Intensities are controlled by the dimensions of these targets, and the amount of the beam impinging upon them. The secondary particles, produced in interactions of the beam with targets placed at different locations around the accelerator ring, feed the different beams used in experiments.

From a particular target, the secondary particles pass through the beam transport sections leading to the beam separator stages and beam shaping sections. These beam transport sections consist of series of dipole and quadrupole magnets, which focus the beam and select particles of the correct momentum for the experiment fed by that beam. By the time the beam reaches the first electrostatic separator, it consists of a stream of particles moving parallel to each other and with approximately the same momentum. The beam separator, by means of crossed electric and magnetic fields, picks out particles with a particular velocity which, since all particles have approximately the same momentum, amounts to picking out particles of a particular mass. After refocusing and a second momentum selection, the beam passes through the second separator stage and then into the beam shaping section which distributes the beam for uniform coverage of the detection device in which the interactions are to take place.

C. Specifics of this Study

For this experiment, the beam consisted of 2.7 BeV/c antiprotons, while the detection device was the 20" Shutt Bubble Chamber filled with hydrogen. This paper is a report of multipion production in antiproton-proton annihilations. In particular, it is a study of the annihilation of

antiprotons with protons into six charged with or without one or more neutral pi mesons, i.e.,

$$\bar{P} + P \rightarrow 3\,\pi^{+} + 3\,\pi^{-} + n\pi^{o}$$

where n could conceivably be any number up to 13, but is rarely more than two.

The collection and identification of events of this type will be described, along with a brief description of the process involved in converting the photographs of tracks left in the bubble chamber to usable data. The observed characteristics of these final states, i.e.,

$$\bar{P} + P \rightarrow 3\,\pi^{+} + 3\,\pi^{-} + n\pi^{o} \quad , \quad n = 0,\ 1,\ 2 - - -$$

will be presented and an attempt to explain them will be made. Of prime interest among these are the cross sections, angular distributions and angular correlations.

Finally, the results of a search of the data for resonances will be set forth and compared with those from other experiments.

II. DATA PROCUREMENT

A. Beam Properties

In any experiment in which a beam of particles is extracted from an accelerator, there is a chance of beam contamination. The experiment under study here made use of a 2.7 BeV/c beam of antiprotons which, though electrostatically separated, could have contained pions, muons, and kaons. The kaons are short-lived and the muons do not interact strongly so the pi mesons are the only contaminant of concern.

To estimate the degree to which mesons were present in the antiproton beam, a delta ray analysis was performed. This is a search of the beam tracks for delta rays, tracks left by electrons scattered from the hydrogen atoms by passing particles. Since the radius of curvature of a delta ray can be related to the mass of the passing particle, increasing with decreasing mass, pion contamination would be indicated by large radii delta rays.

As a check on this analysis, all zero prong, two vee events were examined for evidence of the reaction

$$\pi^- + P \rightarrow \Lambda^o + K^o \quad .$$

None were found! The delta ray analysis resulted in an estimate of beam purity at $99^{+1.0}_{-1.5}\%$, and the complete absence of the aforementioned πP interaction, though a less accurate test, supported the delta ray analysis with a calculated beam purity at least as great.

At the time of the experiment, the beam momentum was believed to be exactly 2.7 BeV/c, but a careful check at the University of Colorado placed

the momentum at 2.68 BeV/c, within $\pm 2\%$, a value which helps to explain the shifted missing mass distributions of the six and seven pion final states.

The average antiproton flux into the Bubble Chamber, i.e., the average number of beam tracks per picture is 11.89.

B. Event Collection

All of the film making up the Iowa State University group's share of the total exposure was scanned for six-prong events. This amounted to 43,553 "good" pictures. The scanners were instructed to look for the topology: one incoming track and six outgoing tracks, hence, the designation "six-prong".

Acceptable events were restricted to a limited region of the chamber. This was mainly to assure that good measurements could be made of the events and partly so that the cross sections could be corrected in a consistent and well-defined manner.

To estimate scanning efficiency, a second scan of the film was undertaken. From the results of the two scans it is believed that only about 4.6% of the six-prong events have been lost.

A total of 2005 six-prong events were found. Of this number, 79 were eliminated at the scanning tables as being unmeasureable. Such a decision resulted if the events were obscured or the tracks too faint to follow. The remaining 1926 events were recorded on measuring lists for measurement on precision measuring engines.

C. Processing of Events

The Itek precision measuring engines use a precision film stage coupled to Datex encoders to accurately record the positions of tracks relative to

fixed fiducial marks in three different views, corresponding to three different camera positions. This information is stored on punched cards to be later submitted to a spatial reconstruction computer program which calculates positions, angles, and momenta, as well as their associated errors for all measured tracks. The events for which satisfactory reconstructions could be made were submitted to a second computer program which successively tried to kinematically fit the reconstructed tracks to all particle assignments permitted by the conservation laws of the strong interactions.

The routines used for spatial reconstruction and kinematical fitting were DATPRO and GUTS, respectively; DATPRO originating at Brookhaven and GUTS at Berkeley, with some modifications having been made at Iowa State University. The events which did not satisfactorily reconstruct, i.e., events which completely failed reconstruction or reconstructed, but gave indications of mistakes in measuring or unreasonable errors on "good" tracks were remeasured.

After all kinematical processing was completed, the events fell into six categories. The six categories with the criteria determining each and the number of events falling in that category are as follows:

(1) <u>6π category-177</u>
$\chi^2_{6\pi} < 15$, possessed no seven pion fit with $\chi^2_{7\pi} < 5$ and $P_{\pi o} < 100$ MeV/c.

(2) <u>7π category-569</u>
$\chi^2_{7\pi} < 5$, χ^2 for six pion fit > 15, no other four constraint fit.

(3) 6π, 7π ambiguous category-35

Possessed fits to both six pion and seven pion final states with $\chi^2_{6\pi} < 15$ and $\chi^2_{7\pi} < 5$. In addition, this category contains a few events whose χ^2 values for the two fits did not satisfy the above criteria but which were included because their missing masses strongly favored fits rejected on χ^2.

(4) 7π, K fit ambiguous category-40

These events have one or more fits to final states involving kaons as well as seven pion fit, with $\chi^2_{k\ fit} \simeq \chi^2_{7\pi}$.

(5) Large missing mass, no fit category-867

Events with a satisfactory reconstruction but no kinematical fits other than nonunique fits to kaon final states.

(6) Failures-202

Failed to achieve a reasonable reconstruction after two measurements.

Note: No account has been made for 36 events. This group is composed of events fitting uniquely to kaon final states. The sample is somewhat restricted, since the events were required to satisfy the criterion that no track had an error on it's momentum greater than the momentum itself. In part, because of the small number of events achieving unique strange particle fits, but mostly because of the uncertainty as to the validity of these fits, this sample was used only to help estimate upper limits on kaon final state cross sections.

It must be emphasized that the criteria above were chosen to give high confidence levels for the exclusion of contamination from the six and seven pion final states and so are necessarily stringent. The resulting losses of events from the 6π and 7π samples were taken into account for the calculation of cross sections, as will be seen in the next section.

D. Final State Classification

1. 6π category

Because of the difficulty of "faking" a four constraint fit, the 6π sample was thought to be relatively free from contamination. The chi squared and missing mass distributions shown in Figures 1(a) and 1(b), respectively, tend to support this. The solid curve on the chi squared graph is the expected four constraint chi squared distribution. The agreement between the data and the theoretical curve is quite good for the χ^2 distribution, but the missing mass distribution is shifted slightly below the expected value of zero. This is explained in part by the shifted value of the beam momentum.

To determine to what degree, if any, the six pion sample was contaminated with final states possessing one or two π^o's (no more than two π^o's were considered because it was thought that this contamination would be negligible), two different three body effective mass distributions and two different five body effective mass distributions were fit to a superposition of the corresponding three and five body effective mass distributions expected from phase space for six, seven, and eight pion final states. The effective mass distributions chosen were ones free from any resonance activity that might bias such a fit. The resulting percentages of six, seven, and eight pion final states were averaged over the four different fits, giving $100^{+0.0}_{-3.2}\%$, six pions, $0^{+3.2}_{-0.0}\%$ seven pions and 0% eight pions with a χ^2 of 67 for 46 degrees of freedom.

2. 7π category

Figures 1(c) and 1(d) are the chi squared and missing mass distributions for the seven pion sample of events with the solid curve on the chi

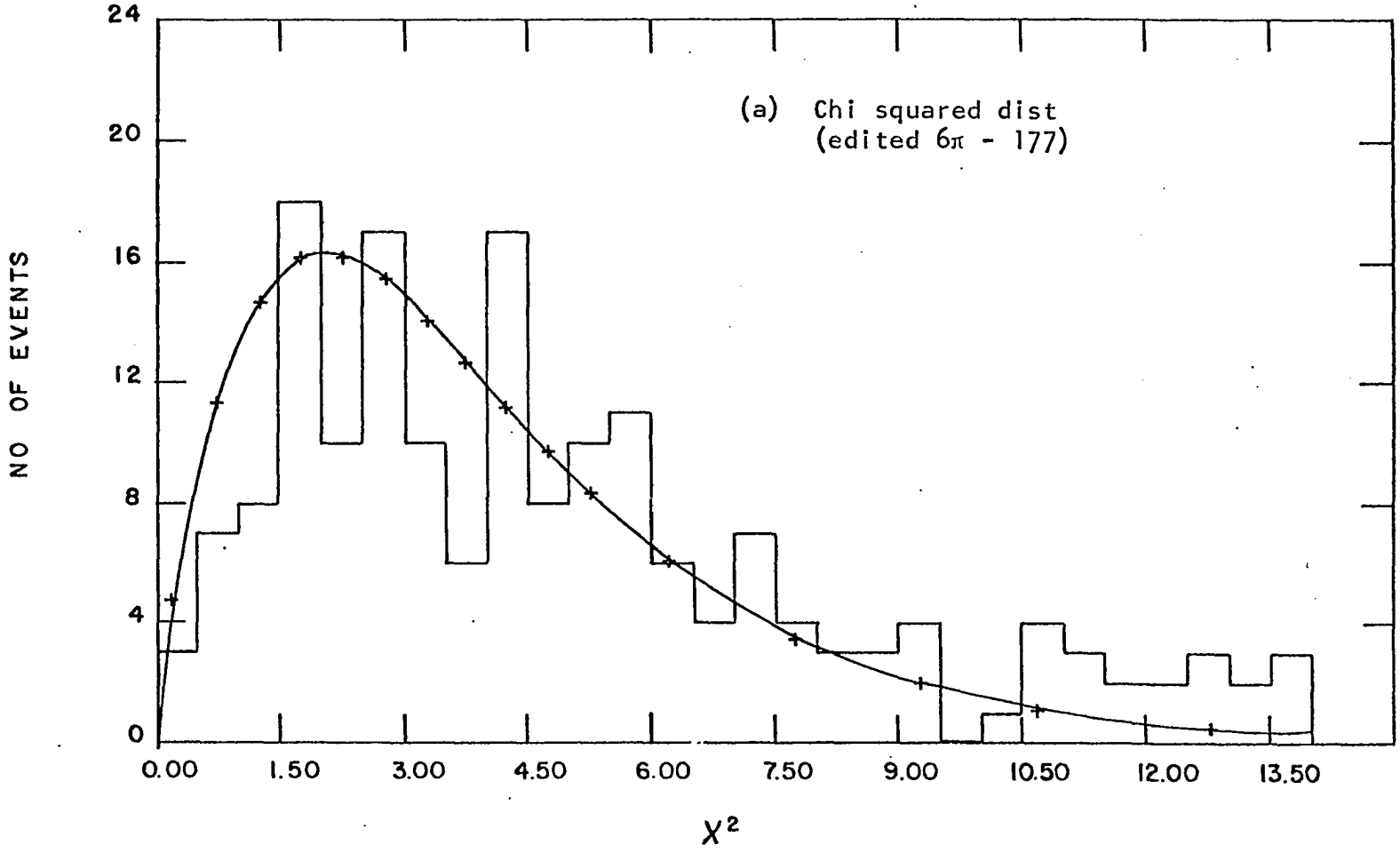

Figure 1a. Chi squared distribution for 6π samples

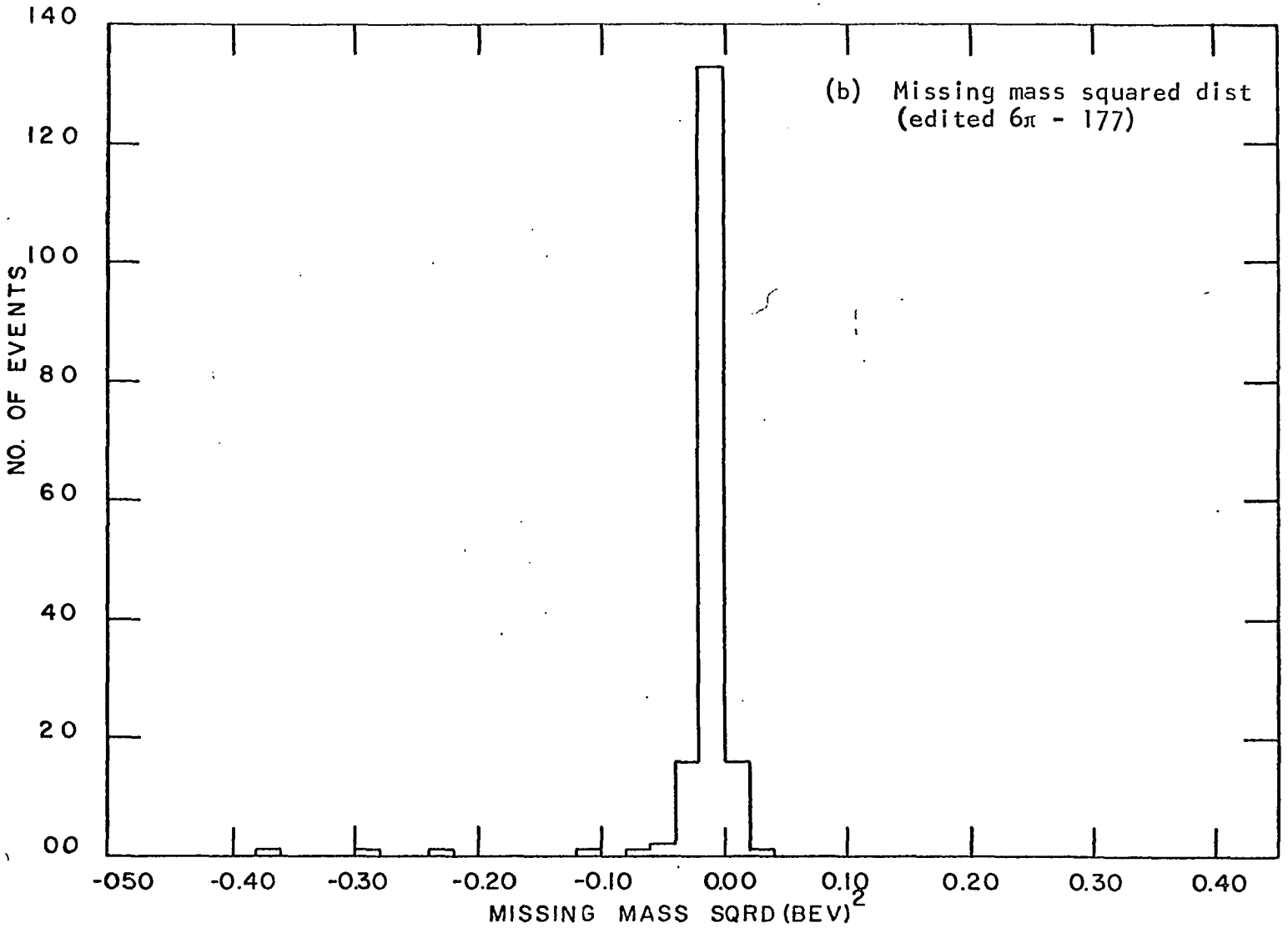

Figure 1b. Missing mass squared for 6π samples

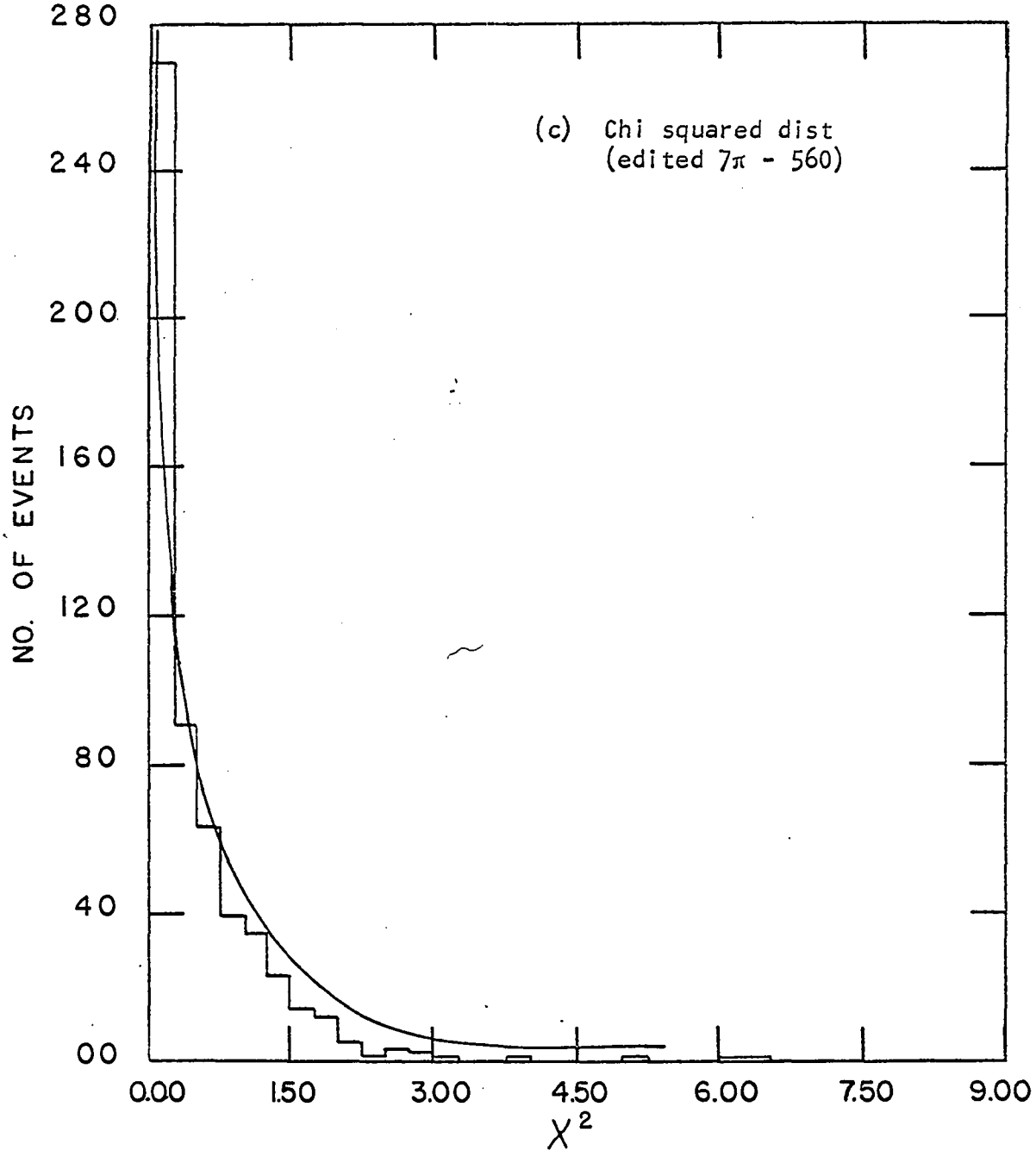

Figure 1c. Chi squared distribution for 7π sample

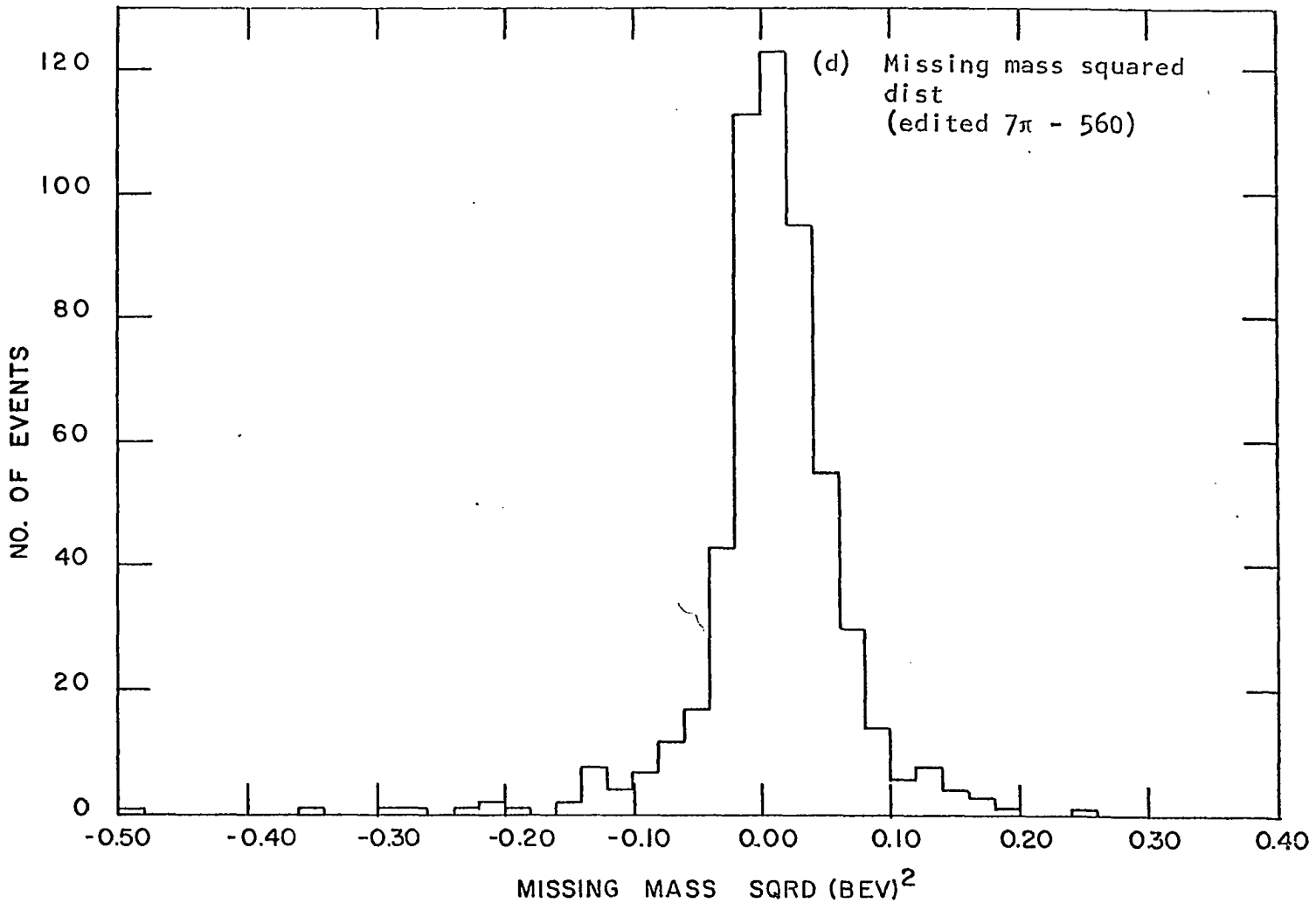

Figure 1d. Missing mass squared distribution for 7π samples

squared plot again representing the theoretical chi squared curve, this time for one constraint. The 7π χ^2 distribution closely follows the expected distribution, but, as for the 6π sample, the missing mass distribution is shifted to lower mass. This shift is again assumed to, in part, be the result of the slight error in the value taken for the beam momentum.

Unlike a four constraint fit in which there are four separate constraining relations between the parameters, strictly determining them and making an accidental fit by an incorrect final state very difficult, the one constraint fit has only one constraining relation to check the measurement. With only one constraining relation for the parameters to satisfy, the probability of an accidental fit is increased. The ease with which a one constraint fit can be "faked" makes contamination of the 7π sample much more likely than for the 6π sample. As with the 6π sample, four different three and five body effective mass distributions were fit to a superposition of phase space curves. The best fit achieved had a χ^2 of 50 for 45 degrees of freedom and the composition; $4.2 \pm 2.5\%$ 6π, $94.8 \pm 4.0\%$ 7π, and $1^{+3.0}_{-1.0}\%$ 8π. Again, contamination due to the final states

$$\bar{P} + P \rightarrow 3\pi^+ + 3\pi^- + n\pi^o, \; n \geq 3$$

was considered negligible.

In neither of these first two categories has any mention been made of possible contamination due to final states involving particles other than pions. The reason for the omission of such searches is that at this momentum, 2.7 BeV/c, the cross sections for K meson production and the production of four or more pions without annihilation are sharply reduced

compared with those for the annihilations modes into multiple pion final states. This is supported by the observation that there are no fits to the final states

$$\begin{aligned}\bar{P} + P &\rightarrow \bar{P} + P + 2\pi^+ + 2\pi^- \\ &\rightarrow \bar{P} + P + 2\pi^+ + 2\pi^- + \pi^o \\ &\rightarrow \bar{P} + \pi^+ + 2\pi^+ + 2\pi^- + n \\ &\rightarrow \pi^- + P + 2\pi^+ + 2\pi^- + \bar{n} \quad ,\end{aligned}$$

and because of the great disparity between the masses of pions and nucleons, the possibility of a real proton or neutron "faking" a pion is small. In the case of K fits, only one unique fit is found to the four constraint case

$$\bar{P} + P \rightarrow K^+ + K^- + 2\pi^+ + 2\pi^-$$

and most of the one constraint fits are ambiguous with other one constraint fits to the same or different final states, making a significant contamination from kaon final states unlikely.

3. 6π, 7π ambiguous category

The events falling into the 6π, 7π ambiguous category are represented in the χ^2 and missing mass plots of Figure 2. So that the respective contributions of these events to the 6π and 7π cross sections might be calculated, the seven pion fit one constraint χ^2 is plotted against the six pion fit four constraint χ^2 for the same event in Figure 2a. The solid line represents the line of equal confidence levels for the one constraint and four constraint χ^2's. For an event lying above this line, the four constraint fit has a higher confidence level than the one constraint fit

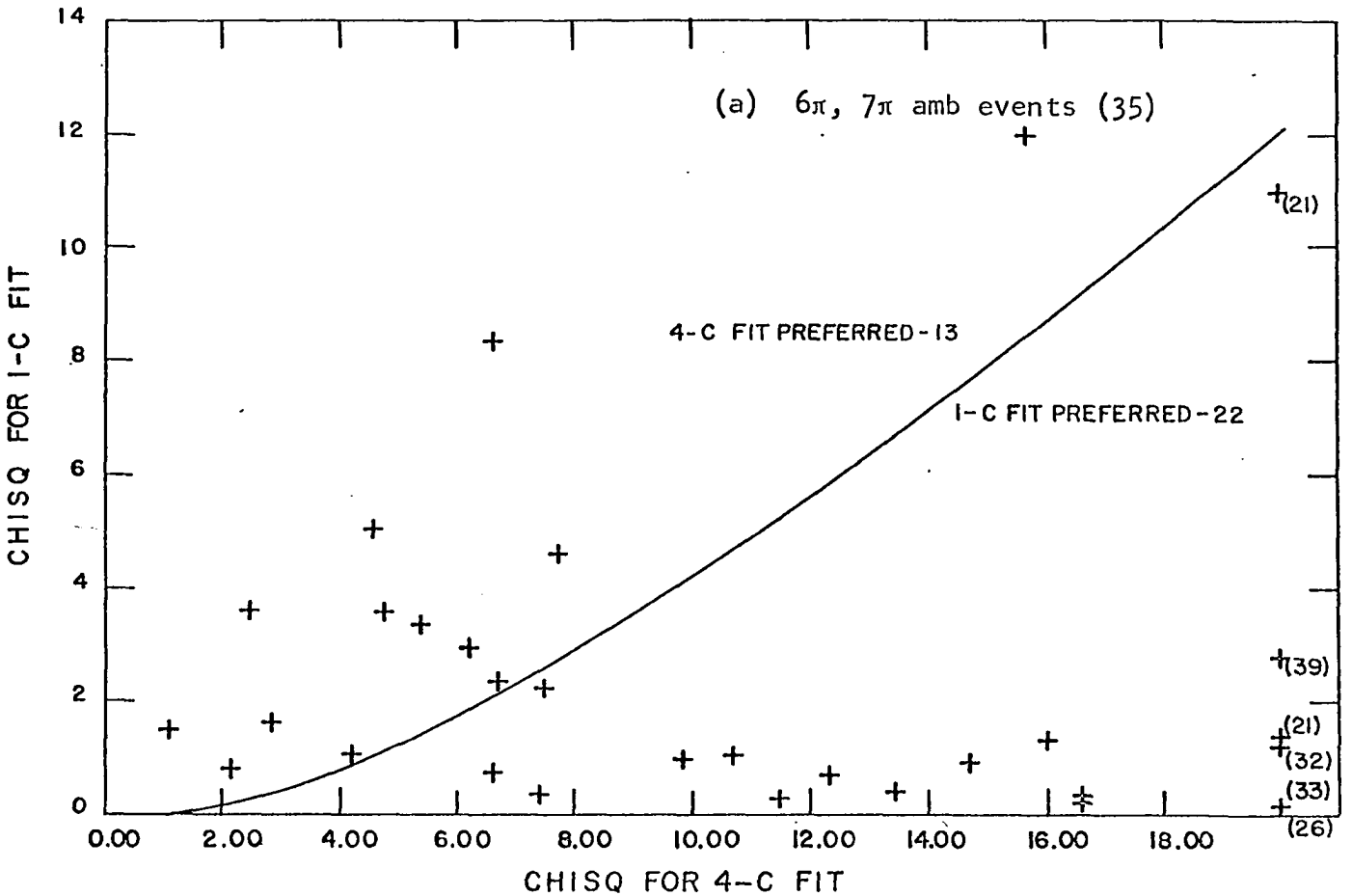

Figure 2a. Chi squared distributions for 6π, 7π ambiguous events

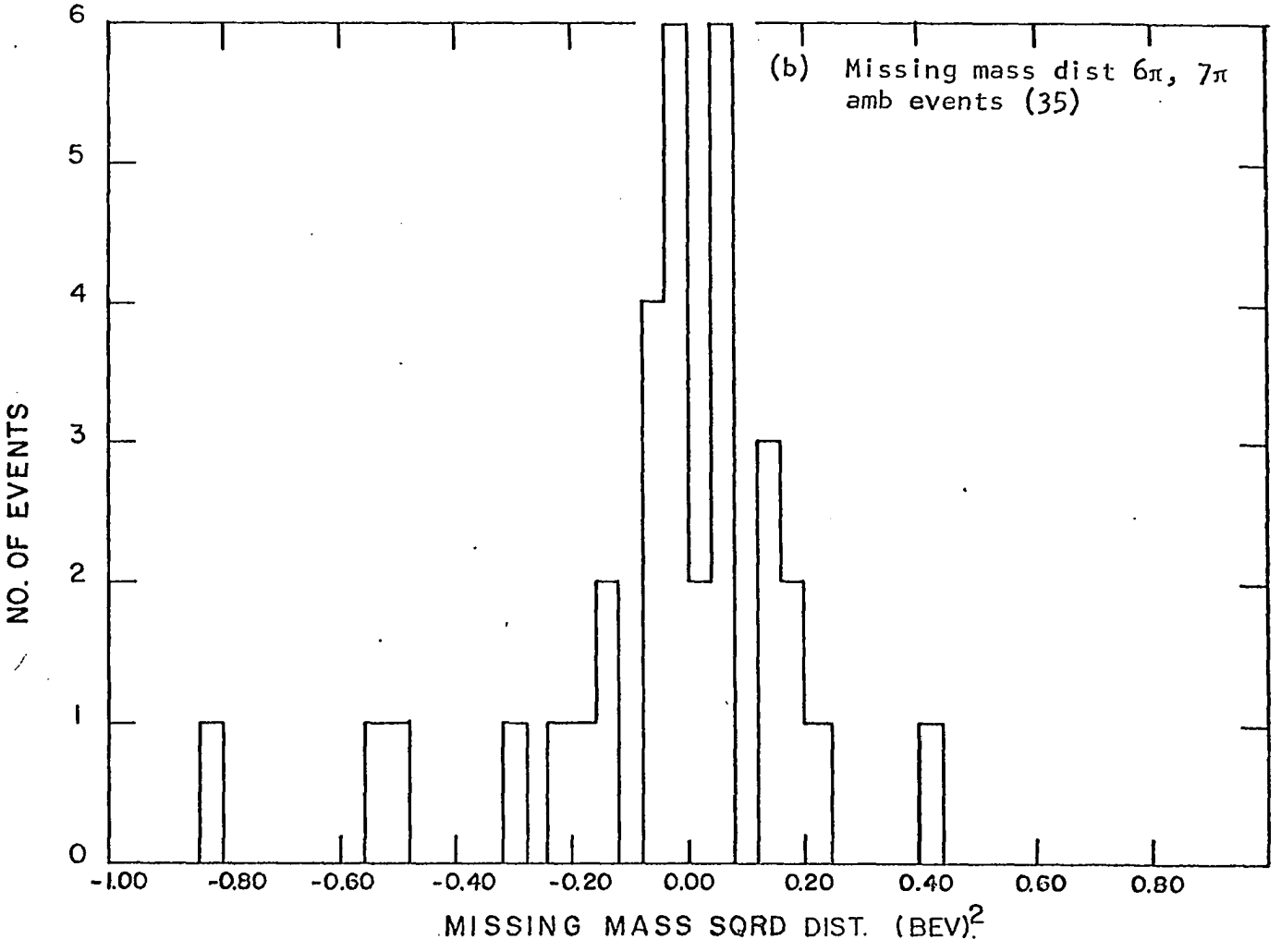

Figure 2b. Missing mass distribution for 6π, 7π ambiguous events

in which case it was classified as a 6π event. The opposite is true for events lying below the line, these events being classified as 7π events.

In this way, the 35 events falling into this class were taken to be 13 6π events and 22 7π events or, 37.1% 6π's and 62.9% 7π's. As a check on this separation, the missing mass distribution of Figure 2b was examined in the following manner. The percentages of events falling above and below zero on the missing mass plot were calculated for the 6π and 7π experimental distributions. From these percentages and the split about zero of 6π, 7π ambiguous events on missing mass, the 6π and 7π contributions could be estimated. The mixture of 6π and 7π events found is consistent with the previous result. Averaging these two results, the distribution of this ambiguous sample was estimated to be $43.4 \pm 15\%$ six pion events and $56.6 \pm 15\%$ seven pion events.

Because of the uncertainty of this separation in regards to particular events, it was decided not to include the events resulting from this separation in the 6π and 7π samples. That this omission did not bias the 6π and 7π samples was checked by an examination of 6π and 7π fits obtained from the separation of the 6π, 7π ambiguous category. This examination revealed no essential differences between the 6 pion fits of the 6π category and those coming from the 6π, 7π ambiguous sample. It was thus felt that the omission of these six pion fits from the 6π category would not alter the character of the results of this study. A similar examination of the seven pion fits revealed a tendency for the π^o to go backward in the center of mass system relative to the antiproton, but again the behavior of these fits in all other respects was such that they were believed to be incapable of biasing the 7π sample by their absence.

4. 7π, K fit ambiguous category

Forty events fit the seven pion hypothesis along with one or more fits to final states with kaons present. These final states are

$$\bar{P} + P \rightarrow K^+ + K^- + 2\pi^+ + 2\pi^- + \pi^o$$

$$\rightarrow K^+ + \pi^- + 2\pi^+ + 2\pi^- + \bar{K}^o$$

$$\rightarrow K^- + \pi^+ + 2\pi^+ + 2\pi^- + K^o$$

and the four constraint case

$$\bar{P} + P \rightarrow K^+ + K^- + 2\pi^+ + 2\pi^- \quad .$$

Since these events often possessed several K fits, which for the most part could not be separated, K fits could not be used to establish a general separation criterion for the entire sample. Consequently, the separation of the 7π, K fit category was based upon the seven pion fits only. For these events it is observed that the effective mass distributions not involving the π^o are shifted to lower mass. This is taken as an indication of the presence of strange particle events. To estimate the number of such events in the sample, the two singly charged three body effective mass distributions were added and compared with the predictions of phase space. This is shown in Figure 3. It is estimated that this plot represents 9 ± 4 K fits and 31 ± 4 7π fits. This estimate was made under the assumption that all excess effective mass combinations below the peak of phase space come from kaon fits. Though very crude, this assumption is probably justifiable considering the uncertainty surrounding the validity of the K fits in this data.

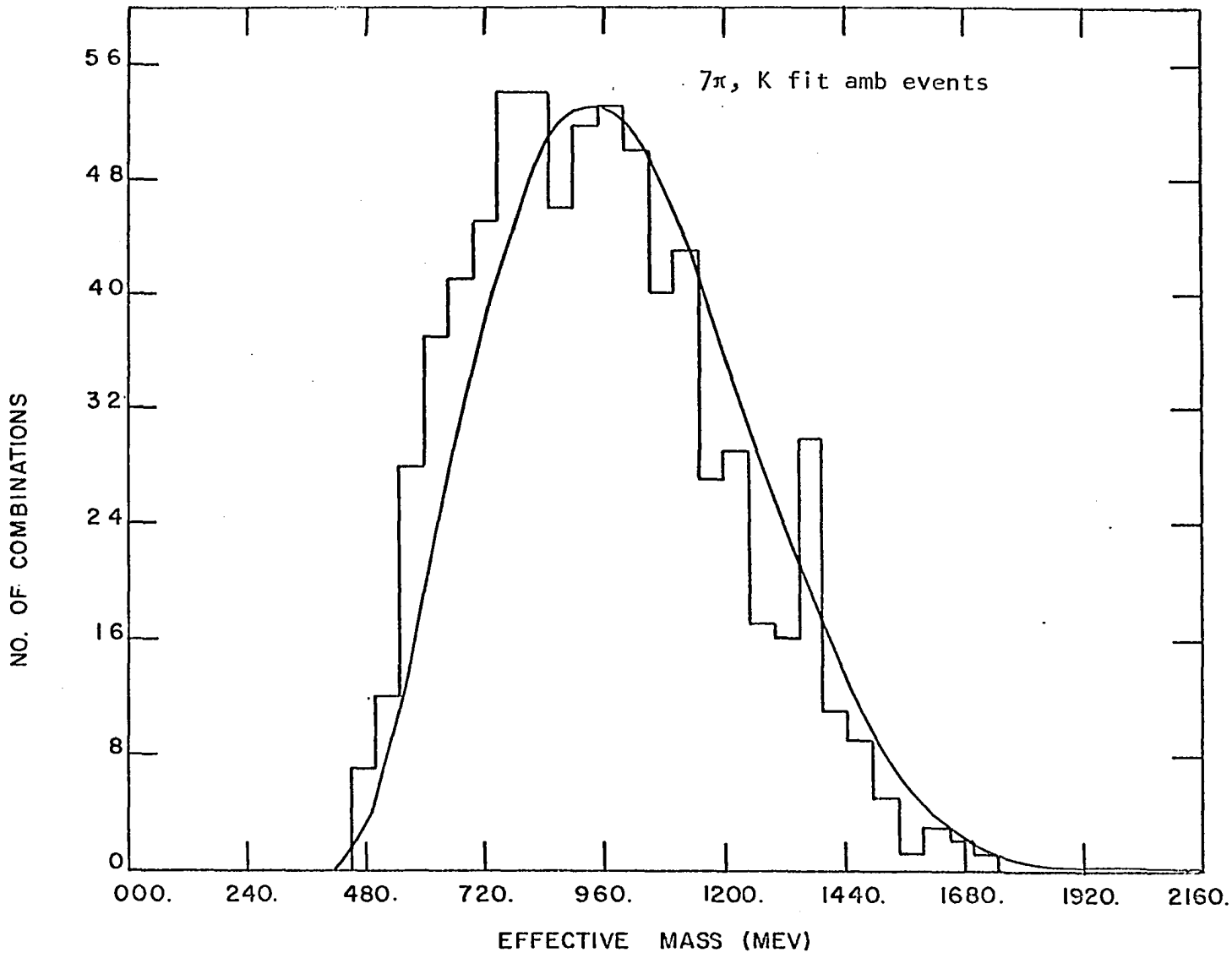

Figure 3. Three-body effective mass distribution for seven pion fits to events from 7π, K fit ambiguous category

5. Large missing mass, no fit category

This category contains all events with satisfactory reconstructions not falling in the previous four categories. This includes a large number of events which did not attempt, because of unfavorable missing masses, or failed to achieve a fit, as well as a large group of events with high missing masses ($\gtrsim$300 MeV) possessing nonunique one constraint fits to the kaon final states

$$\bar{P} + P \rightarrow K^+ + K^- + 2\pi^+ + 2\pi^- + \pi^o$$

$$\rightarrow K^+ + \pi^- + 2\pi^+ + 2\pi^- + \bar{K}^o$$

$$\rightarrow K^- + \pi^+ + 2\pi^- + 2\pi^+ + K^o$$

In most cases, when an event has one K fit, it will have several more, often to the same final state. That is, an event will have several fits to the same final state, merely changing the track or tracks to which K's have been assigned. When problems like this arise in achieving a satisfactory fit it often indicates the presence of more than one neutral particle. Hence, the assignment of kaons to one or more tracks is often just an attempt to account for excess energy really being carried off by another π^o and the event, in fact, belongs to one of the unconstrained final states

$$\bar{P} + P \rightarrow 3\pi^+ + 3\pi^- + n\pi^o$$

where n is greater than or equal to two. In support of this observation is the small number of unique four constraint fits. Such fits are significantly more reliable than one constraint fits. There was only one unique

fit to

$$\bar{P} + P \rightarrow K^+ + K^- + 2\pi^+ + 2\pi^- \quad ,$$

so that K fits do not constitute a serious contaminant.

Because the number of events belonging to kaon final states is believed to be small, the missing mass distribution (Figure 4), representing all the events of this category, was fitted to a superposition of four curves; (1) the experimental 6π missing mass distribution, (2) the 7π sample missing mass distribution, (3) the effective mass phase space distribution for $2\pi^o$'s out of eight pions and (4) the phase space distribution for the effective mass of $3\pi^o$'s out of nine pions. Since the uneven nature of the missing mass distribution made this fit somewhat crude, only the resulting percentage of unconstrained final states is given, no attempt being made to separate these into eight and nine pion final states. The best fit to the data was achieved with a mixture of $16.2\pm5.0\%$ six pion events, $17.4\pm5.0\%$ seven pion events, and $66.4\%\pm10.0\%$ events with eight or more pions. Because the fit was quite poor, an attempt to check these numbers was made in fitting the three and five body effective mass distributions for these events to superpositions of the corresponding phase space distributions for six, seven, eight and nine pions. Though the fits for both distributions were still very bad, they were somewhat better than for the missing mass distribution.

The fit to the three body effective mass distribution gave a significantly lower contribution from eight pions, making up for this in part by a greatly increased nine pion percentage; however, the results from fitting the five body effective mass distribution were entirely consistent with

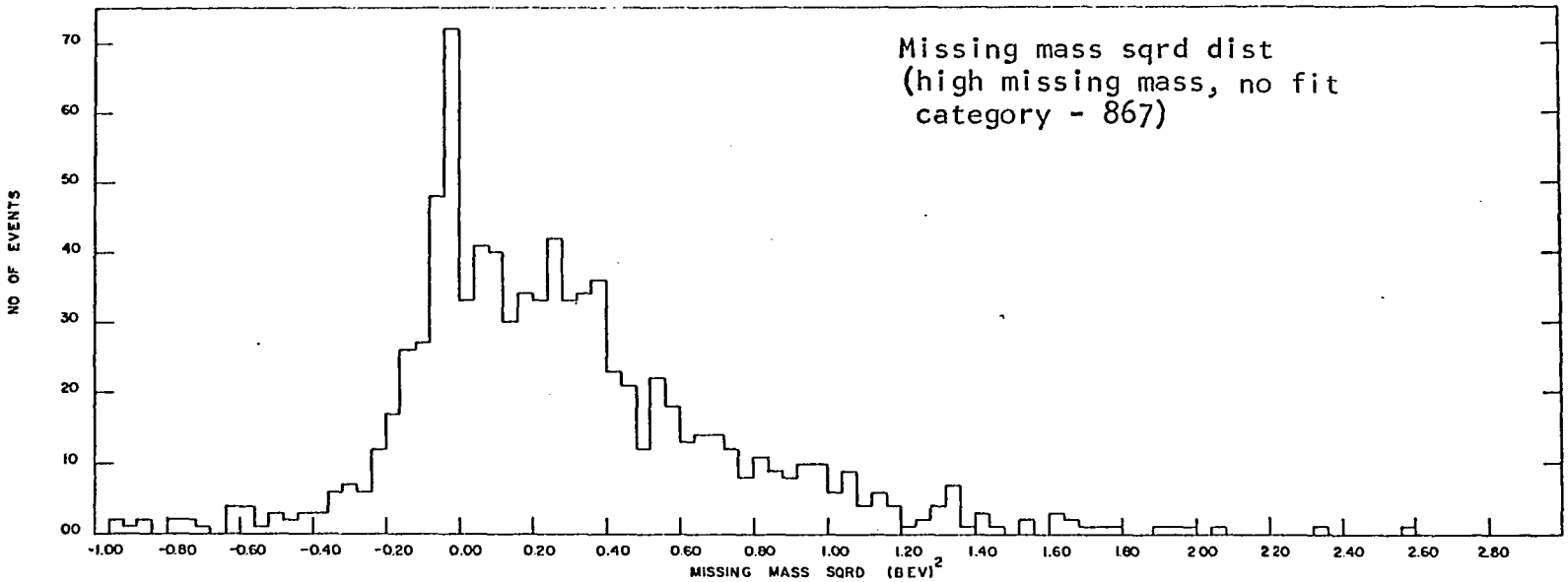

Figure 4. Missing mass distribution for all events in large missing mass, no fit category

those from the missing mass distribution fit.

6. Failures

This category consists of the events that after two measurements failed to achieve a satisfactory reconstruction. These events came principally from two sources: (1) events failing because of mistakes made by the measurer and (2) events which were discarded at the measuring machines as being unmeasurable because of obscuration by beam tracks. Since neither group of events failed because of any peculiarity of the events themselves, it was felt that these events could be taken into account by simple correction to all cross sections. It was also felt that the events failing reconstruction due to the problems associated with the measurement of steeply dipping tracks could be accounted for in an identical manner.

In justification of this assumption, it is pointed out that except for a negligible number of K's, all the tracks would be pions, in which case there is no kinematical reason other than the difference in average pion momentum to favor one or another of the three principal final states. Though the percentage of pions with momentum below 50 MeV in the 7π sample is roughly twice that for the 6π sample, the small number of events involved could hardly effect any significant change in the cross sections.

7. Cross sections

To obtain the cross sections for the various final states observed, the number of events classified as belonging to particular final states had to be individually corrected for contaminations and losses. The new numbers were then all adjusted proportionately for the 202 events in the

failure category and the 79 events discarded earlier as unmeasurable. Finally, the cross sections for all final states were calculated[1] and corrected for scanning efficiency, resulting in Table 1.

Table 1. Cross Sections

Final State	Cross Section
$\bar{P} + P \rightarrow 3(\pi^+) + 3(\pi^-)$	1.05 ± 0.15 mb
$\rightarrow 3(\pi^+) + 3(\pi^-) + \pi^o$	2.18 ± 0.40 mb
$\rightarrow 3(\pi^+) + 3(\pi^-) + n\pi^o,\ n \geq 2$	1.69 ± 0.55 mb
$\rightarrow K^+ + K^- + 2(\pi^+) + 2(\pi^-)$	≤ 0.03 mb
$\rightarrow K^+ + K^- + 2(\pi^+) + 2(\pi^-) + \pi^o$	≤ 0.05 mb
$\rightarrow K^\pm + \pi^\mp + 2(\pi^+) + 2(\pi^-) + K^o$	≤ 0.24 mb
Total for six-prongs	5.08 ± 0.39 mb

These cross sections are not inconsistent with the values given in references (1) and (2) as can be seen by a comparison of the multipion final state values (Table 2).

Table 2. Comparison of cross sections with other experiments

	Xuong & Lynch (1)	Present Study	T. Ferbal, et al. (2)
$\bar{P}$ momentum	1.61 BeV/c	2.7 BeV/c	3.28 BeV/c
6π	1.16 ± 0.1 mb	1.05 ± 0.15 mb	0.9 ± 0.1 mb
7π	1.80 ± 0.25 mb	2.18 ± 0.40 mb	2.7 ± 0.3 mb
8π	1.05 ± 0.25 mb	1.69 ± 0.55 mb	2.4 ± 0.5 mb

[1] Each event corresponds to a cross section of 2.42 μb

III. MOMENTUM DISTRIBUTIONS

This analysis and those to follow in the remainder of this paper are based upon only the selected samples of 6π and 7π events of categories (1) and (2). With each set of results the checks for biases introduced by the use of such restricted samples will be discussed.

A. Pion Momentum Distribution

Figures 5(a) and 5(b) show the momentum distributions in the $\bar{P}P$ center of mass of the positively and negatively charged pion, respectively, for the 6π's. The corresponding distributions for the 7π events are shown in Figures 6(a) and 6(b). In Figure 6(c), the momentum distribution for the π^o's from the 7π final state category is plotted. In all cases, the solid curves represent the phase space predictions.

For both final states, the π^- distribution is identical within errors, with the π^+ distribution and both are in general agreement with phase space. Because identity of the π^- and π^+ momentum distributions is a requirement of CP invariance, a significant disparity between the two distributions would be the source of serious concern. The π^o momentum distribution also agrees well with phase space and with the charged pion distributions with no significant excess of events at low momenta indicating contamination from 6π events "faking" a 7π event with low π^o momentum.

The degree to which these distributions agree with phase space and each other supports the assumption that the selection criteria are reasonable, resulting in acceptably low contamination and losses.

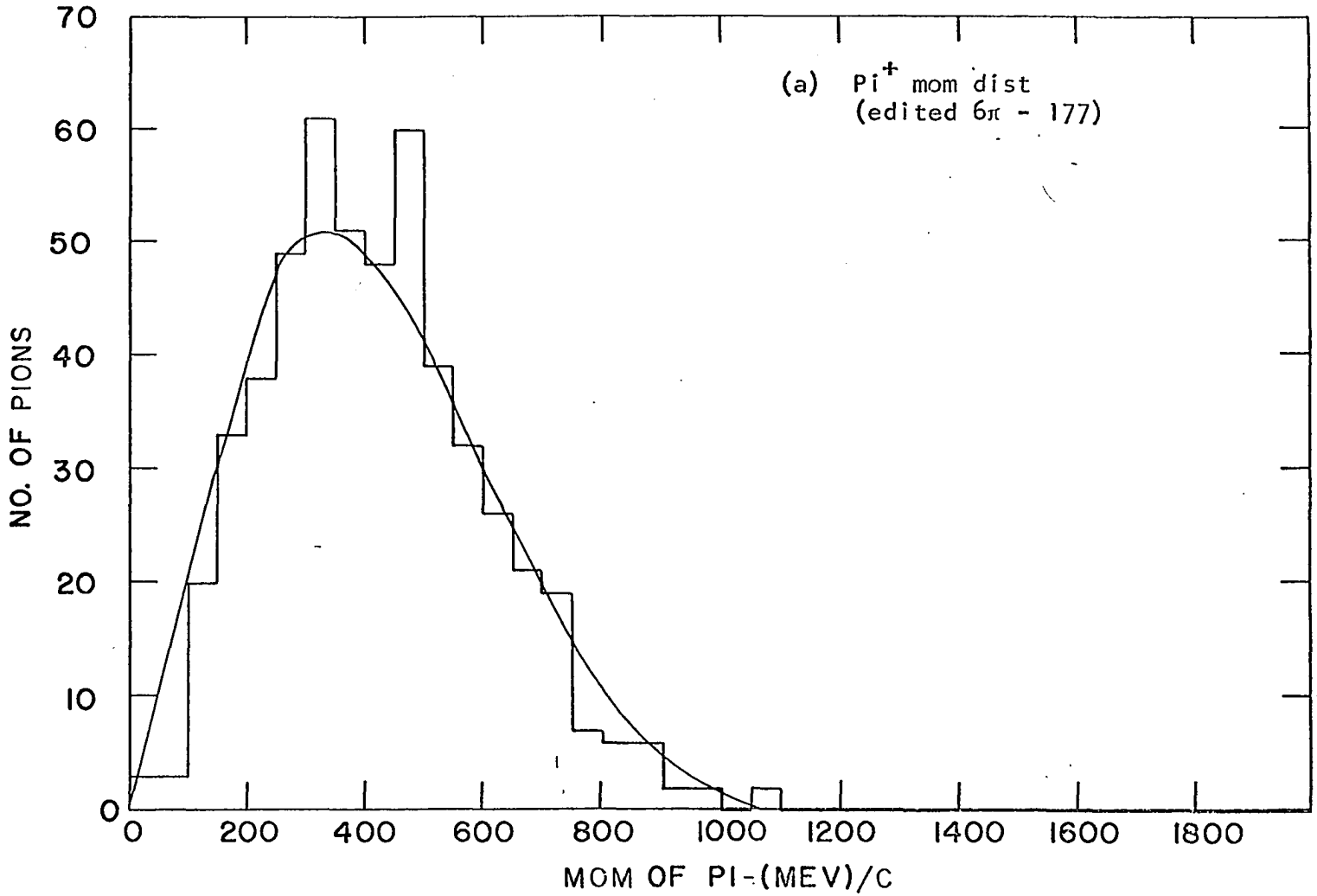

Figure 5a. Center of mass system momentum distribution for pions from events of 6π sample

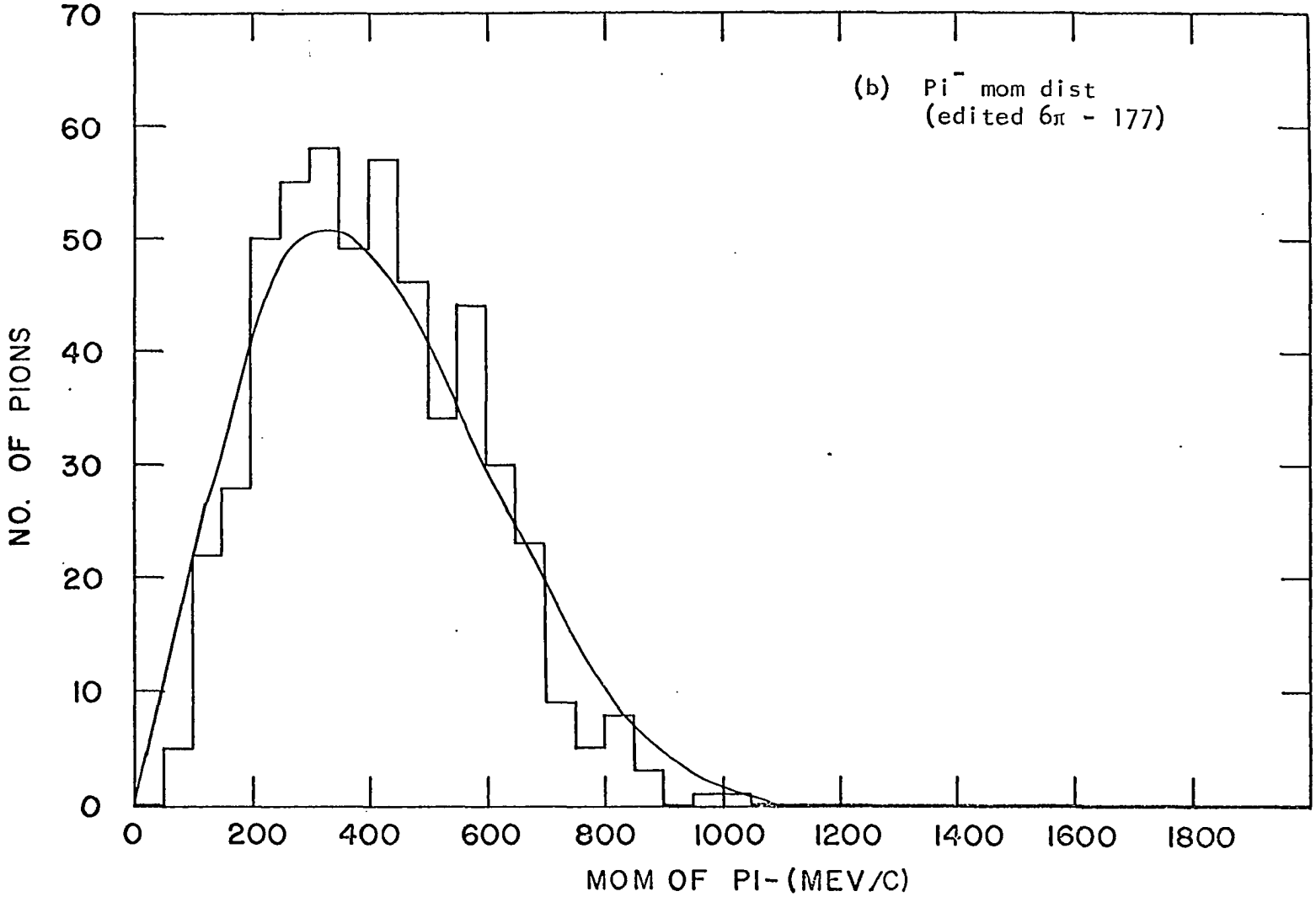

Figure 5b. Center of mass system momentum distribution for pions from events of 6π sample

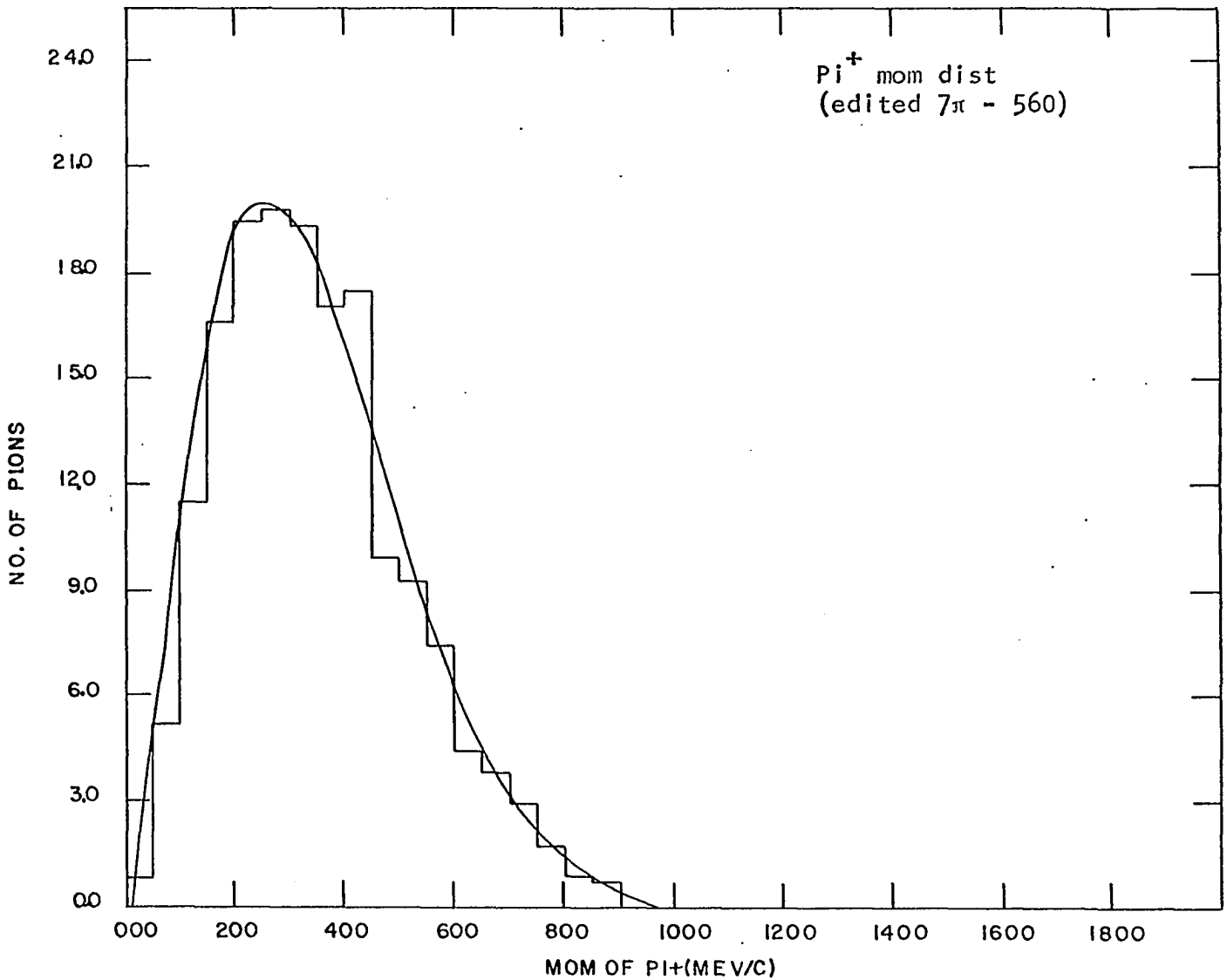

Figure 6a. Center of mass system distribution for pions from 7π sample

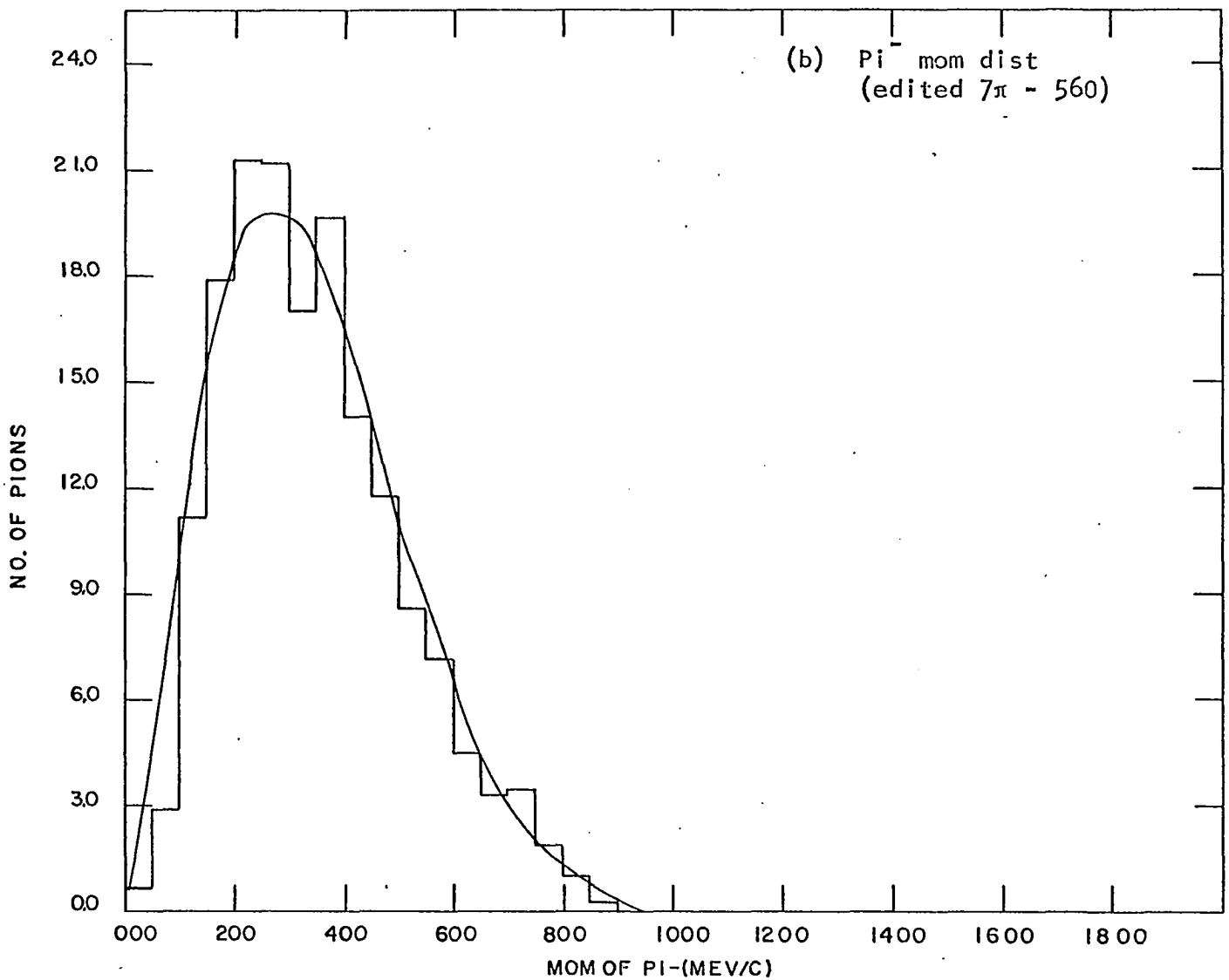

Figure 6b. Center of mass system momentum distribution for pions from 7π sample

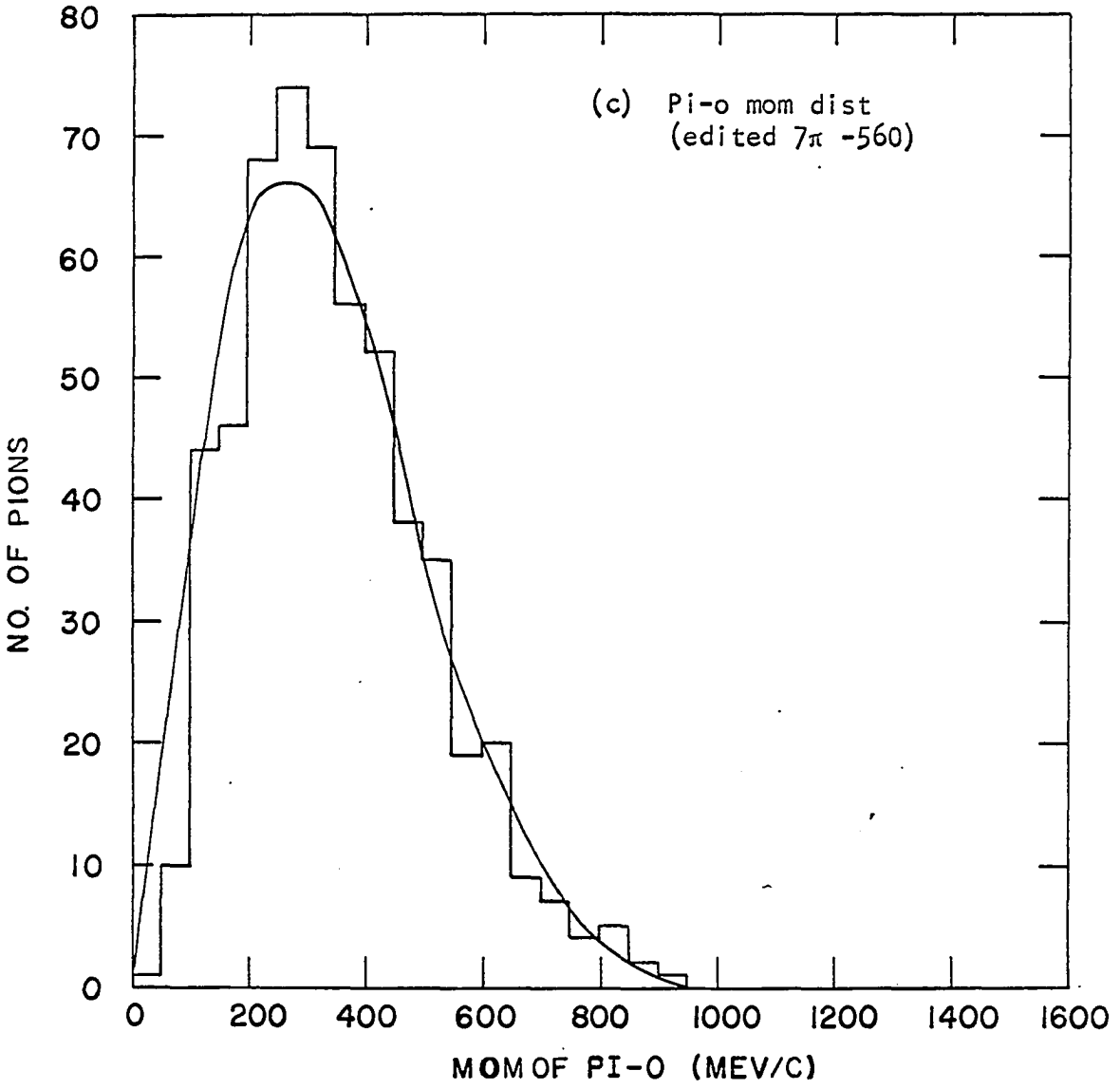

Figure 6c. Center of mass system momentum distributions for pions from 7π sample

B. Transverse Momentum

The transverse momentum for a secondary particle produced in an interaction is the component of its momentum perpendicular to the momentum of the incoming particle. A distribution of transverse momenta is of interest because of its independence from the initial and final states and its relation to the interaction.

Cocconi (3) has suggested that the distribution of transverse momenta for all secondary particles emerging from a proton-proton interaction takes the form

$$f(p_t)\, dp_t = k p_t\, e^{-p_t/\alpha}\, dp_t$$

where k and α are constants. Figure 7 shows the transverse momentum distribution for all measured six-prong events fitted to the above function. The best fit, resulting in a X^2 of 168 for 98 degrees of freedom, is achieved with $\alpha = 0.157 \pm 0.009$ BeV/c.

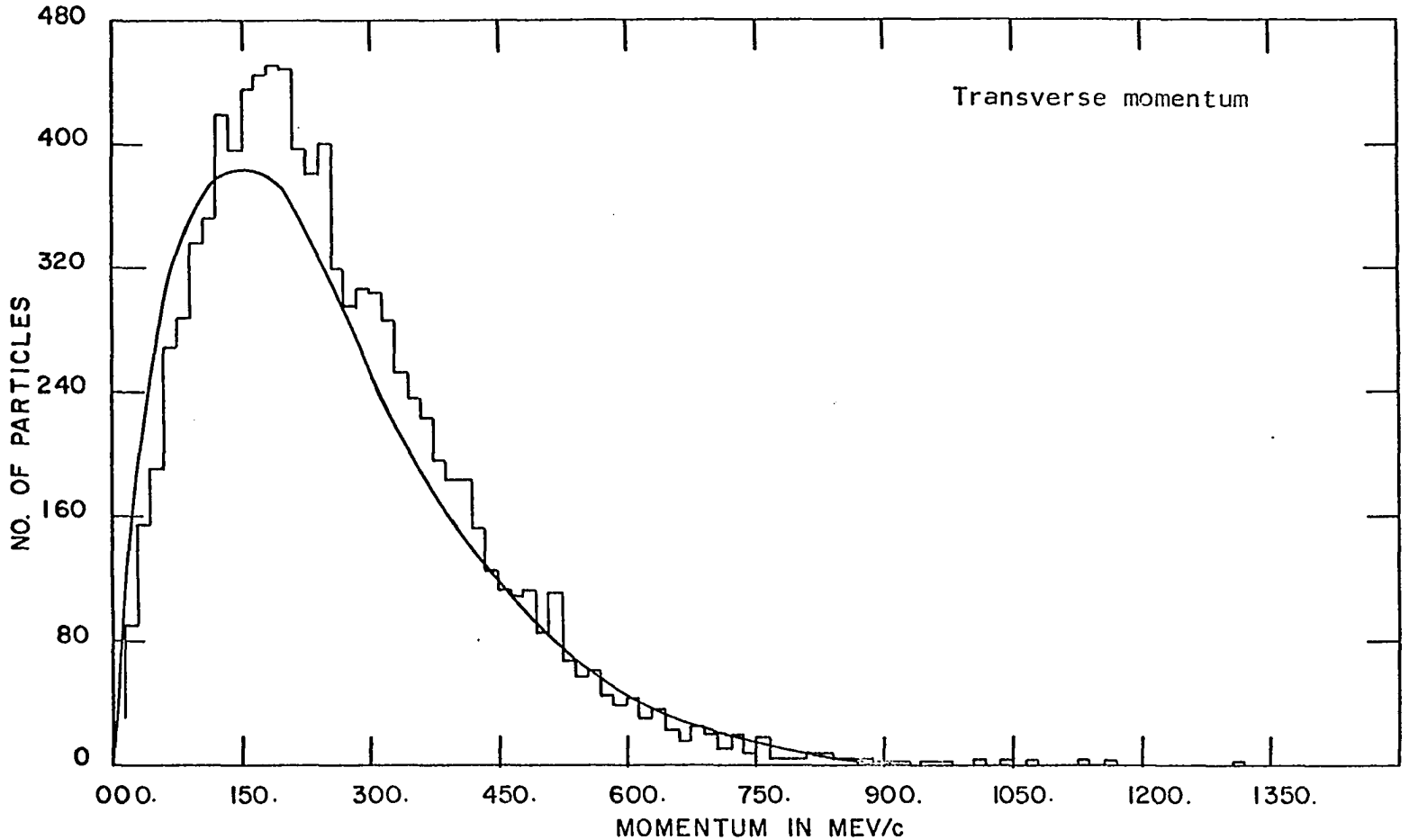

Figure 7. Transverse momentum distribution for all six-prong events which achieved a spatial reconstruction

IV. ANGULAR DISTRIBUTIONS

A. Forward-Backward Ratios

In an effort to explain some of the features of $\bar{P}P$ annihilations, several models have been proposed. One that has been applied with some success is the Koba-Takeda model (4) and its subsequent refinements (5). Briefly, for purposes of calculations a nucleon is thought of as being broken into two regions; a neutral core with a radius of roughly $2/3 \frac{\hbar}{2m_\pi c}$ and an outer pion cloud. The overall charge of the pion cloud gives the charge of the nucleon. In $\bar{P}P$ annihilations, the cores interact, spraying out pions more or less uniformly but the cloud pions tend to maintain the motion they had with their respective nucleons, this motion manifesting itself in the center of mass system as a forward peaking of the negative pions and a backward peaking of the positive pions with respect to the antiproton.

Figure 8 contains the center of mass angular distributions for the charged pions from the 6π events and the charged and neutral pion distributions from the 7π's. Unlike the observed data, the π^o distribution from the 7π sample should be symmetric since the π^o is its own antiparticle and the $\bar{P}P$ strong interaction is invariant under CP. The slight forward peaking of this distribution has been thoroughly investigated and is attributed to the strict criteria under which the 7π sample was chosen. That is, in trying to avoid contamination, many 7π events with low π^o laboratory momentum were lost to other categories. As one would expect, the π^o distributions of 7π fits from the 6π, 7π ambiguous and 7π, K fit ambiguous categories both show backward peaks. Further, when the π^o distribution for all 7π fits is plotted, this asymmetry disappears. To

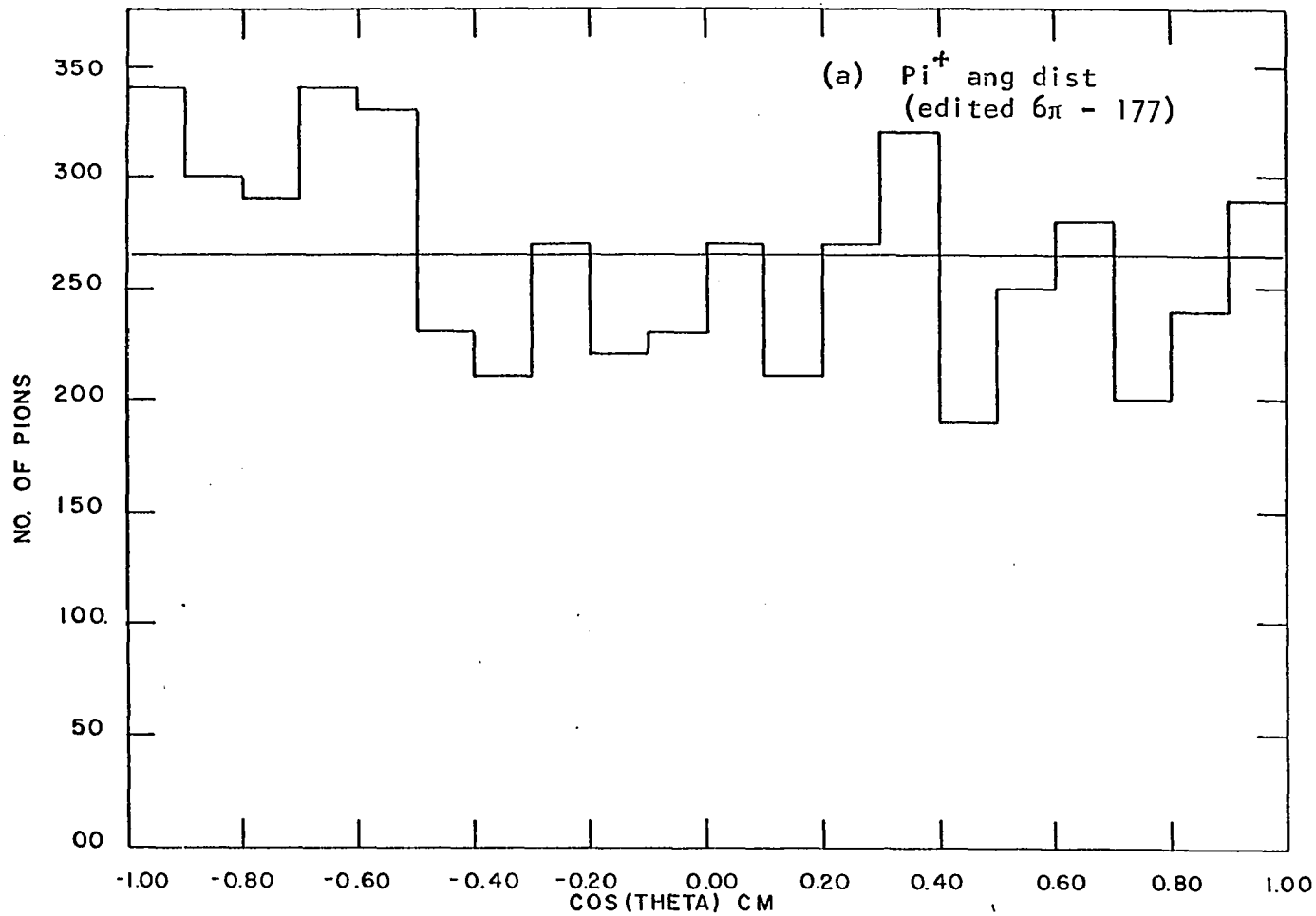

Figure 8a. Center of mass system angular distributions for pions from 6π samples

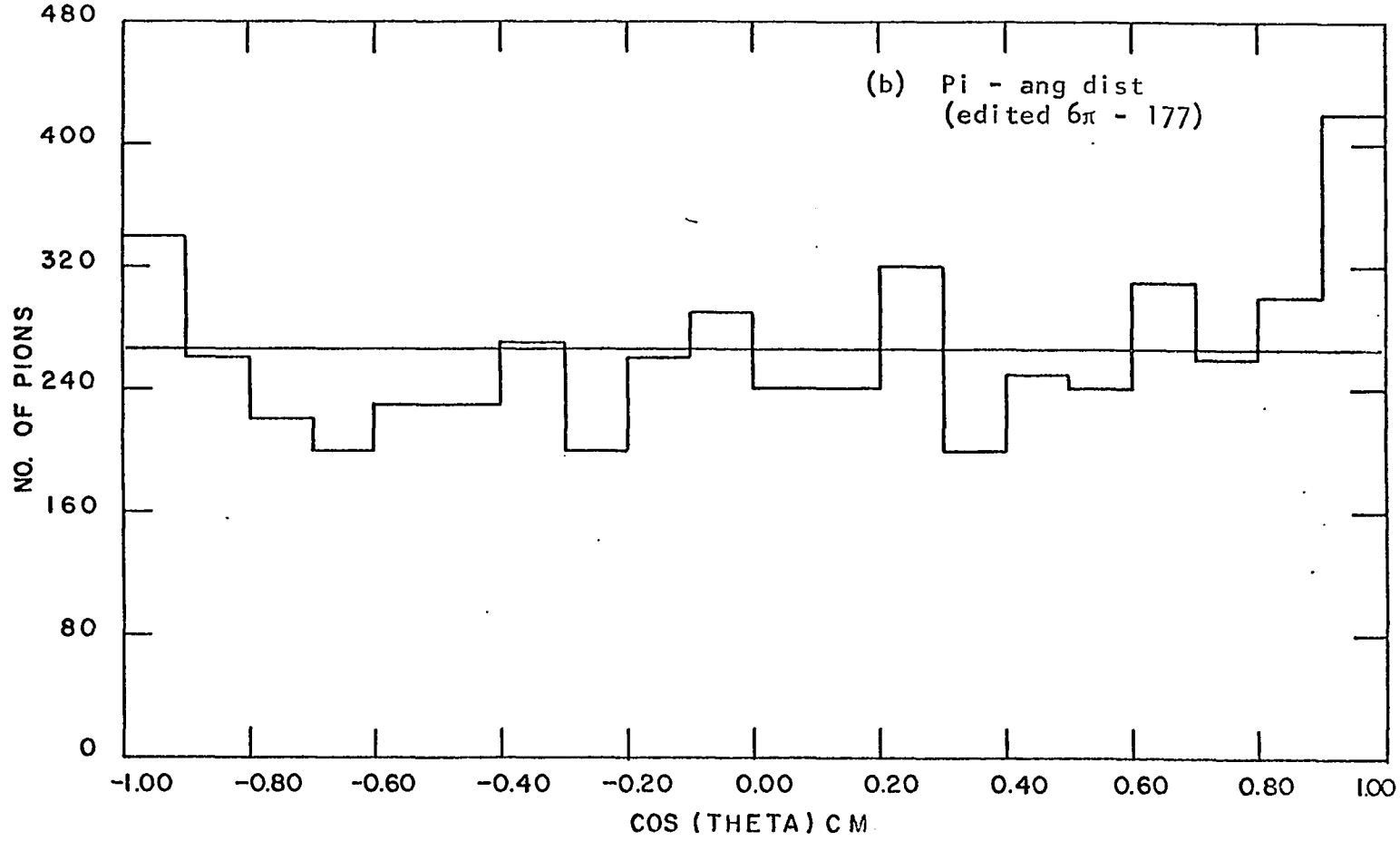

Figure 8b. Center of mass system angular distributions for pions from 6π samples

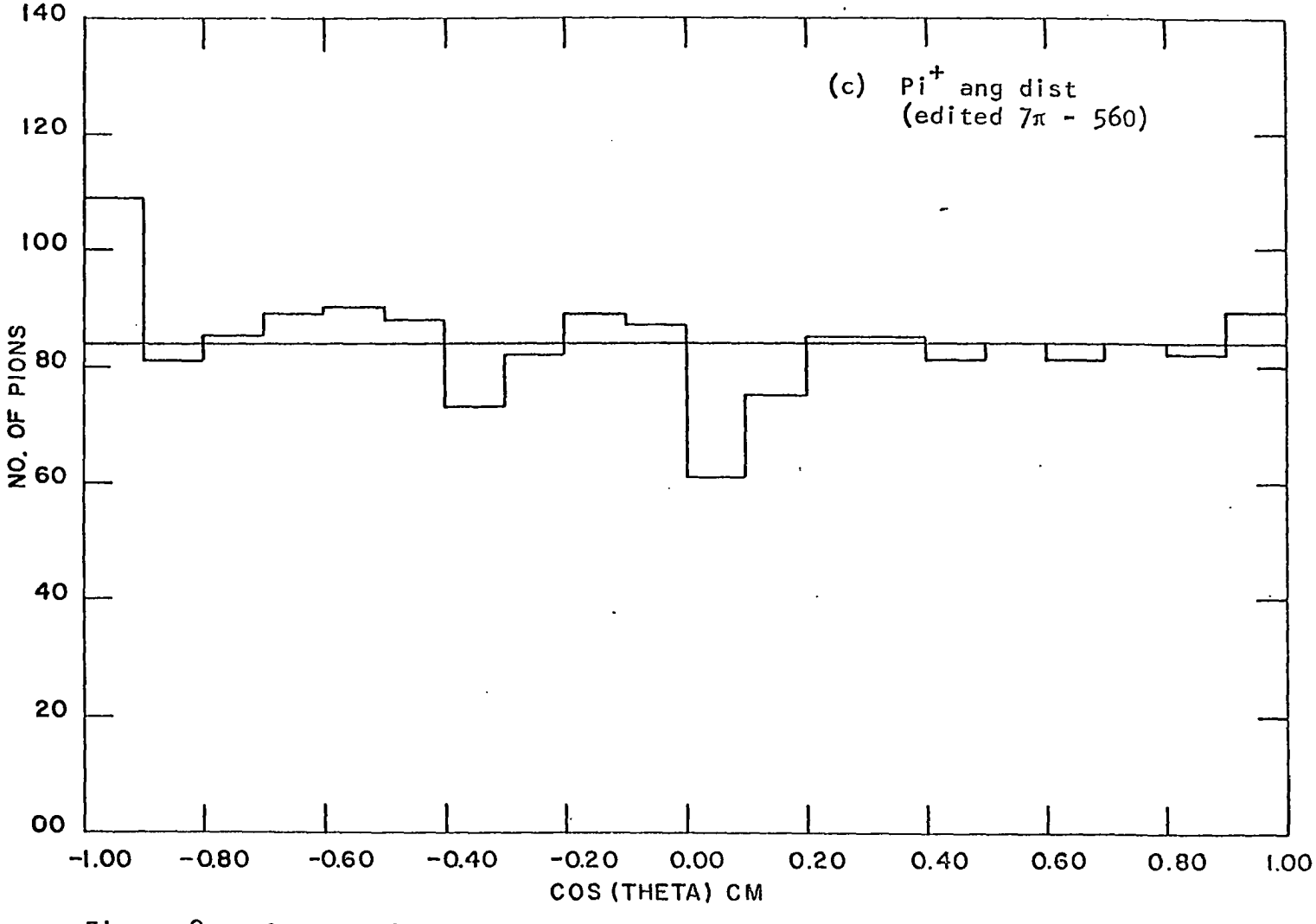

Figure 8c. Center of mass system angular distributions for pions from 7π samples

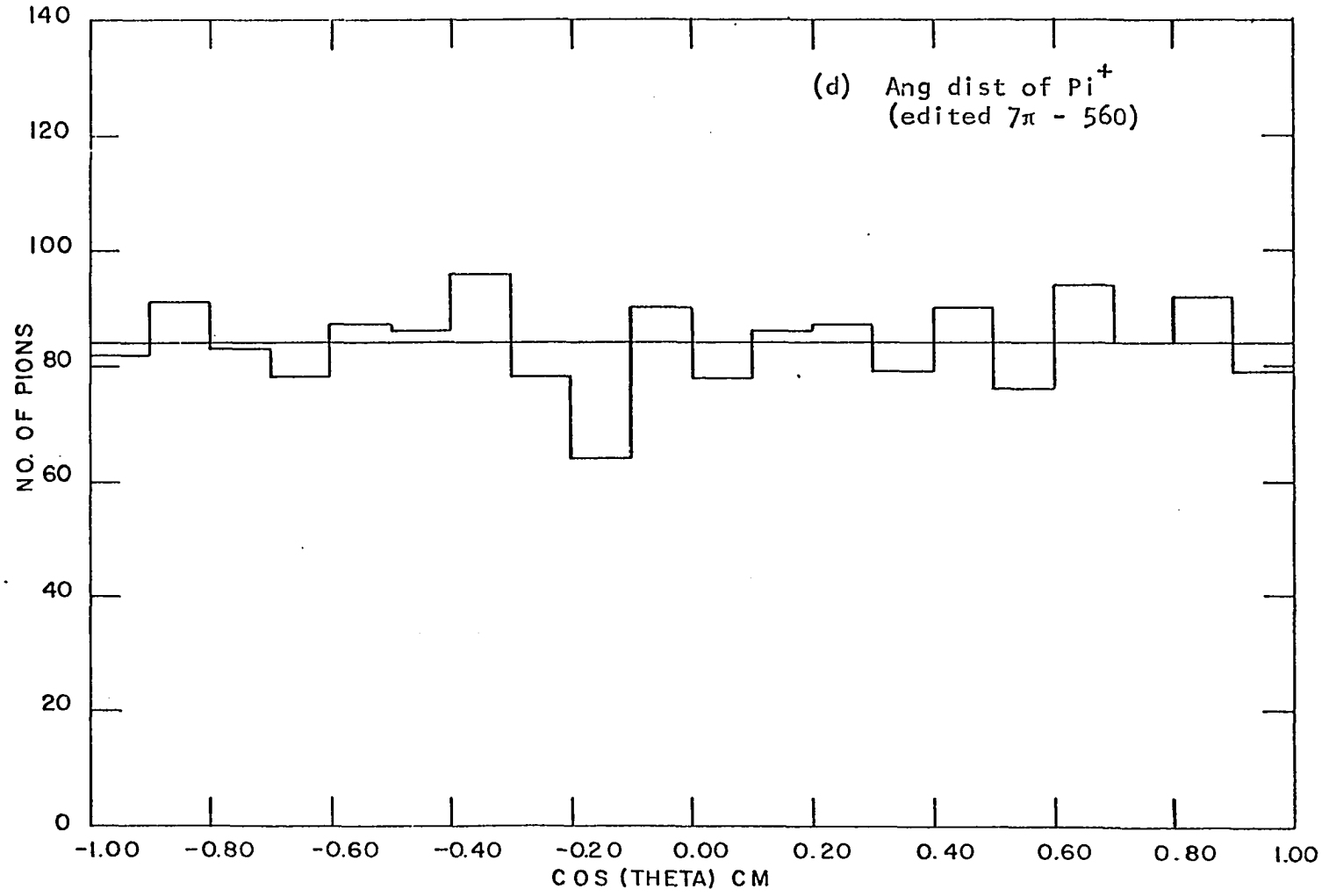

Figure 8d. Center of mass system angular distributions for pions from 7π samples

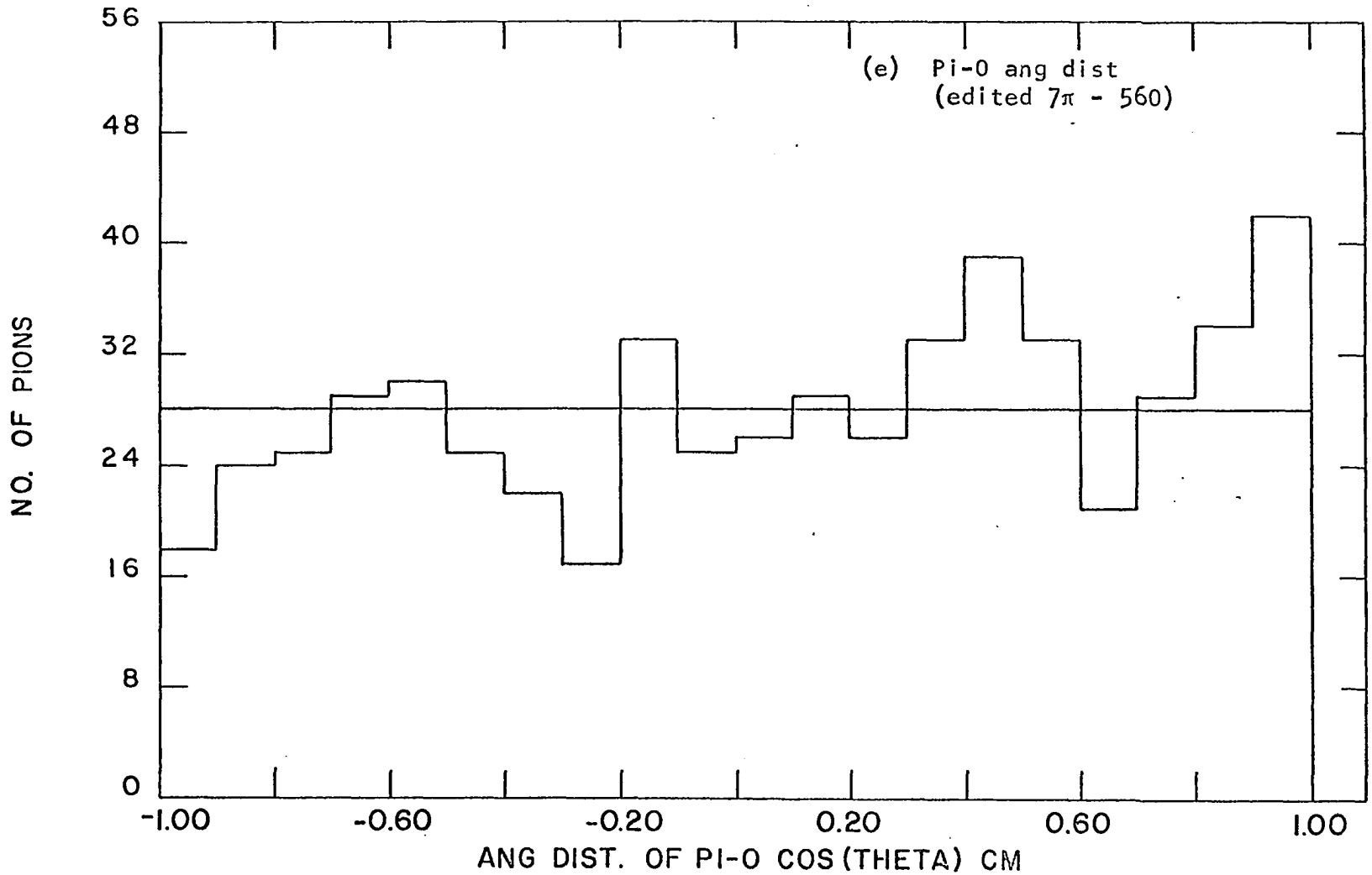

Figure 8e. Center of mass system angular distributions for pions from 7π samples

allay any fears that this asymmetry might be an indication of biases in other data associated with this sample, the 7π fits excluded from the sample were examined in complete analogy with those included, with the result that no essential difference, other than that discussed above, could be found between the two groups of 7π fits.

The charged pions from the 6π events clearly show the peaking described above, the π^- mesons showing a forward peak and the positive pions a backward peak. In the 7π's, on the other hand, the peaking is less evident, though still present. This tendency toward isotropy with increasing multiplicities has been observed by all other investigators of multiple pion production in antiproton-proton annihilations (1, 2, 6) and has been explained, within the framework of the Koba-Takeda model (4), as a "washing out" of effects due to the roughly fixed number of "cloud" pions by the increasing number of "core" pions.

For the purpose of quantitative comparisons, the forward to backward and polar to equatorial ratios have been tabulated. These ratios are defined as $\frac{F-B}{F+B}$ and $\frac{P-E}{P+E}$ where F, B, P, and E have the following definitions:

F: $\cos\theta > 0$

B: $\cos\theta < 0$

P: $\cos\theta < -.5$ or $\cos\theta > .5$

E: $-.5 < \cos\theta < +.5$

In Table 3, the positive pion distribution has been reflected about zero and added to the negative pion distribution.

Table 3. Forward to backward and polar to equatorial ratios for CM pion production angles

Process	$\frac{F-B}{F+B}$	$\frac{P-E}{P+E}$	$\frac{P-E}{P+E}$
6π	0.049 ± 0.021	0.068 ± 0.023	
7π	0.023 ± 0.012	0.024 ± 0.012	0.018 ± 0.021
	charged		neutral

B. Angular Correlations

In Figure 9 are displayed the angular correlations between like and unlike pions in the $\bar{P}P$ center of mass system for both the 6π and 7π final states, gamma representing the angle between pion pairs. The solid curves give the predictions of Lorentz invariant phase space. The data show that like pions tend to be separated by smaller angles and unlike pions by larger angles than phase space predicts. The failure of the angular correlations to agree with phase space as seen in the present data, is supported by the corresponding data in other experiments (1, 2, 6). Goldhaber, et al.(7), have attributed the deviations from the simple statistical model to the influence of Bose-Einstein statistics. Their (7) prediction that the effect should be more significant for lower $\bar{P}$ momenta is borne out by a comparison with other experiments (1, 6). Also, it is expected that the average angle should match that of phase space. That this is the case can be seen from Table 4.

Table 4. Angular correlations between like and unlike pions in the $\bar{P}P$ center of mass

	++ and --	+ -	All Pion Pairs	Phase Space
6π	-0.095 ± 0.025	-0.201 ± 0.040	-0.159 ± 0.030	-0.169
7π	-0.070 ± 0.010	-0.168 ± 0.015	-0.129 ± 0.022	-0.149

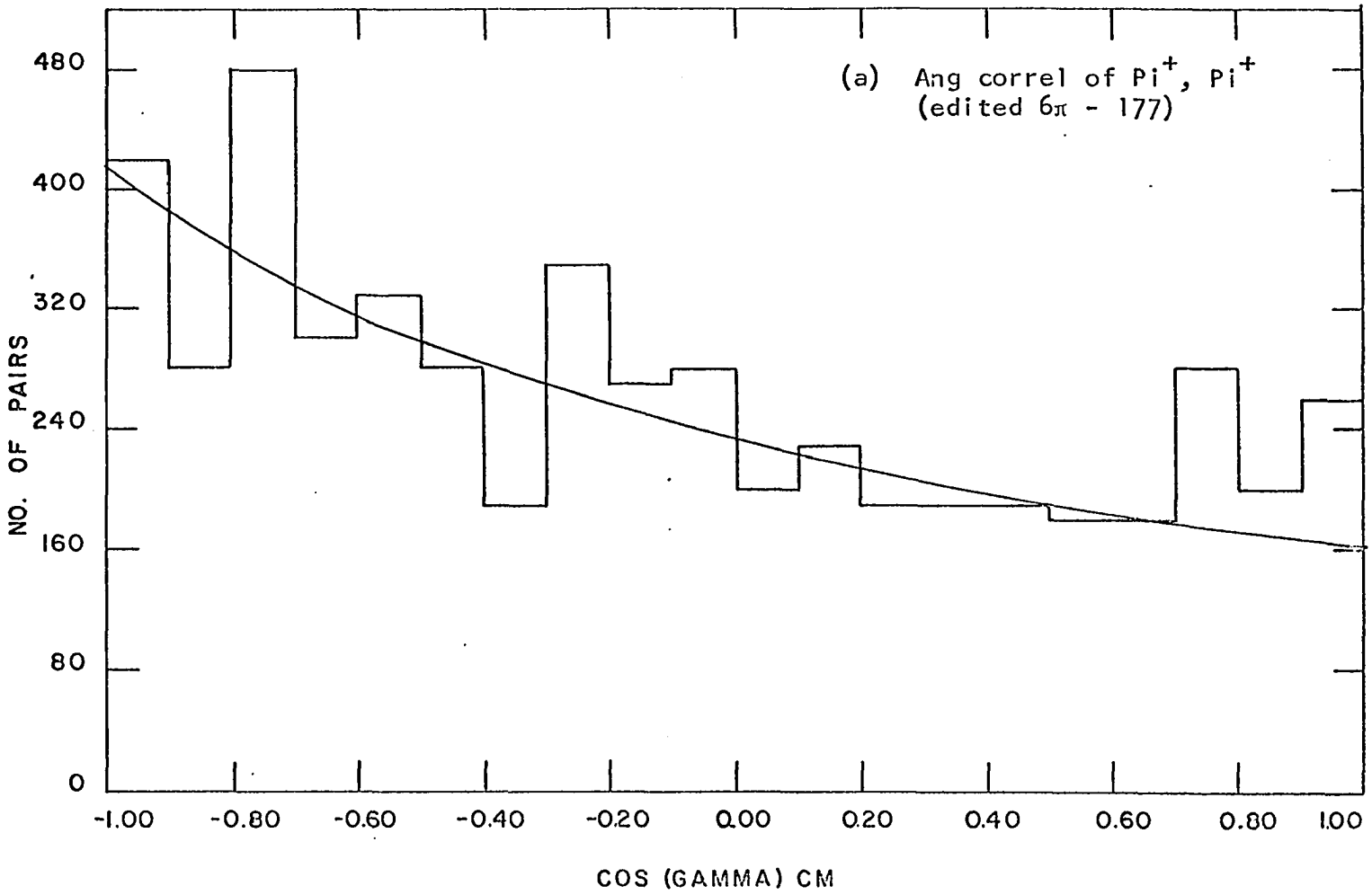

Figure 9a. Angular correlations in the center of mass system for pions from 6π samples

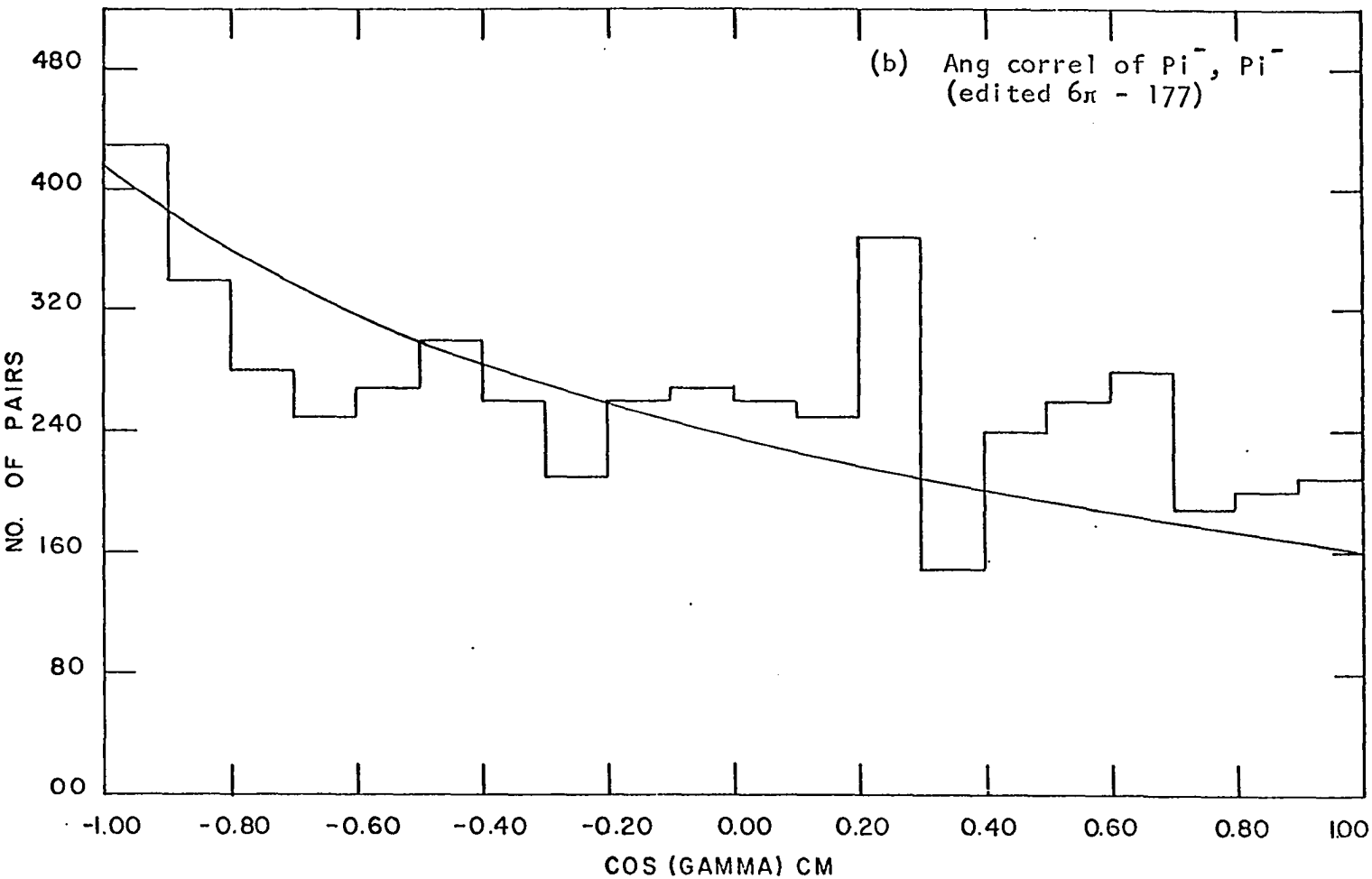

Figure 9b. Angular correlations in the center of mass system for pions from 6π samples

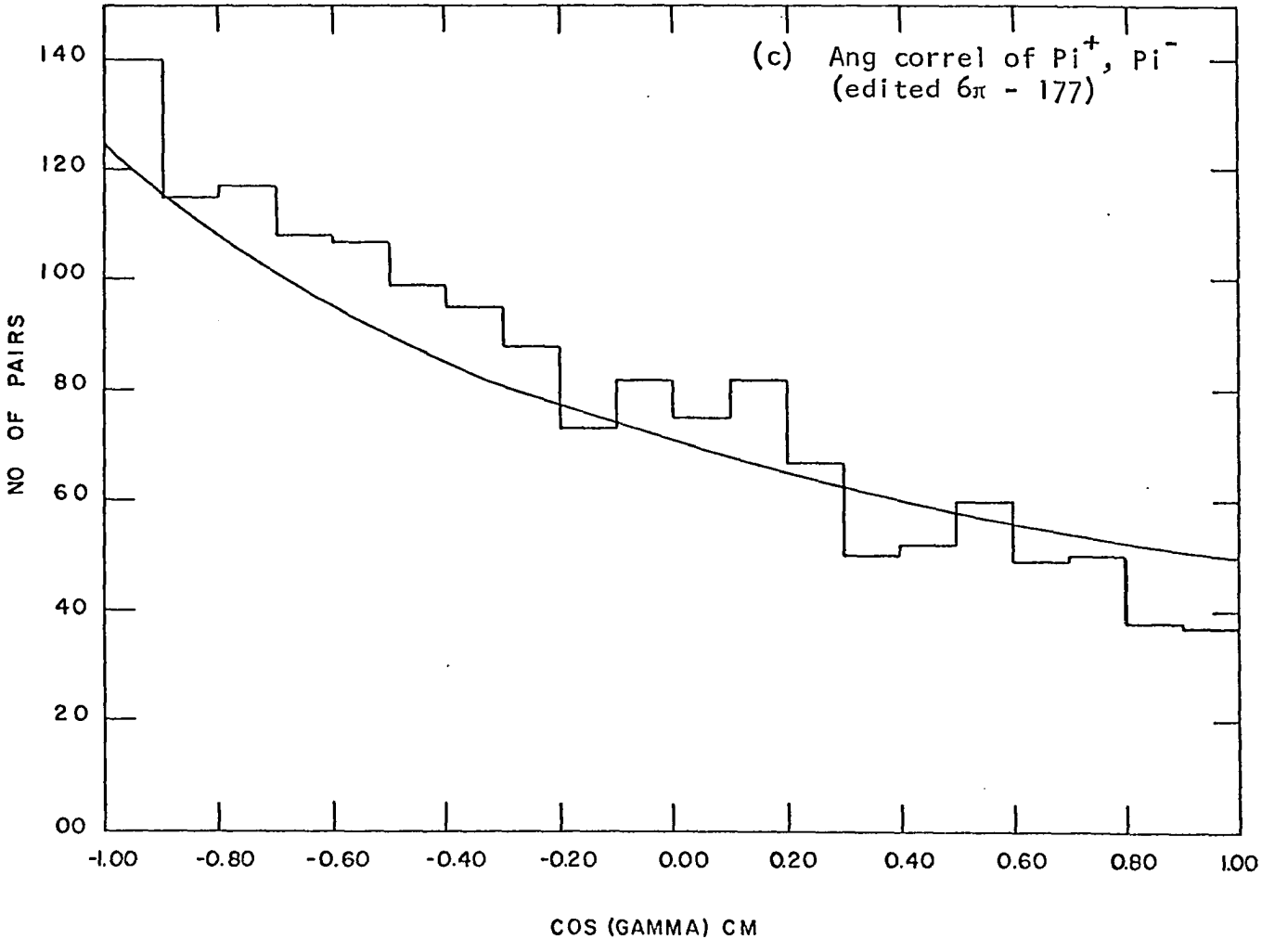

Figure 9c. Angular correlations in the center of mass system for pions from 6π samples

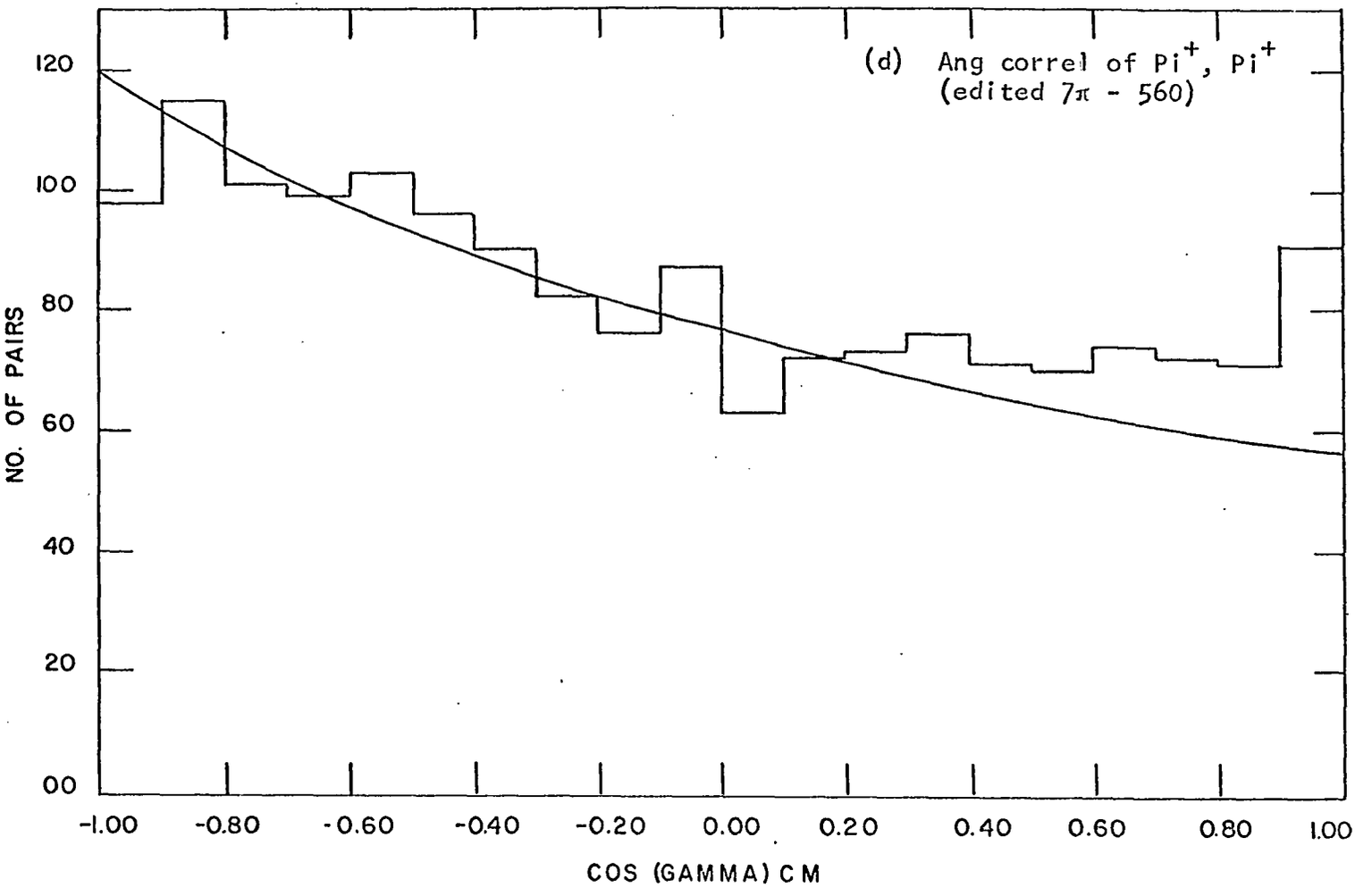

Figure 9d. Angular correlations in the center of mass system for pions from 7π samples

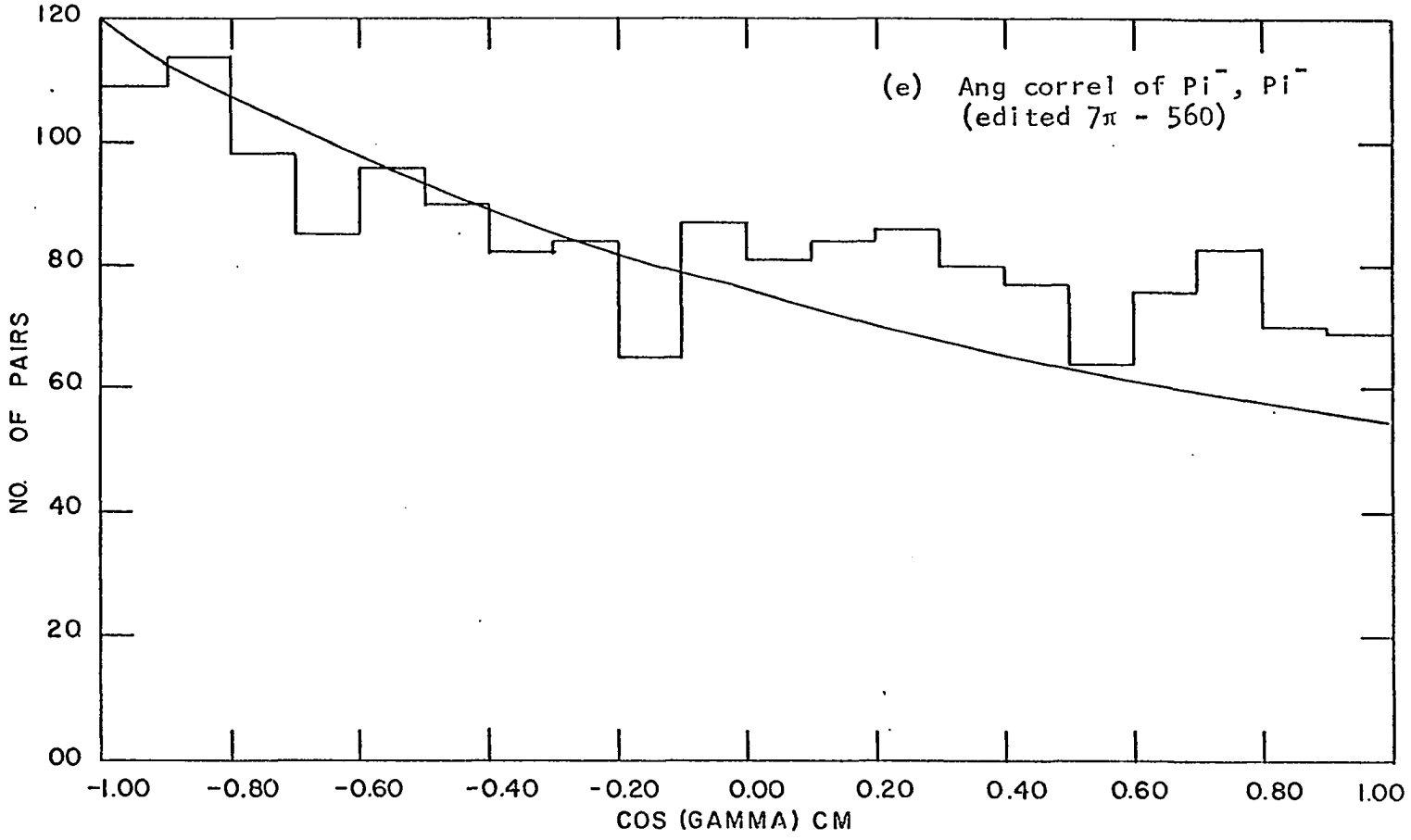

Figure 9e. Angular correlations in the center of mass system for pions from 7π samples

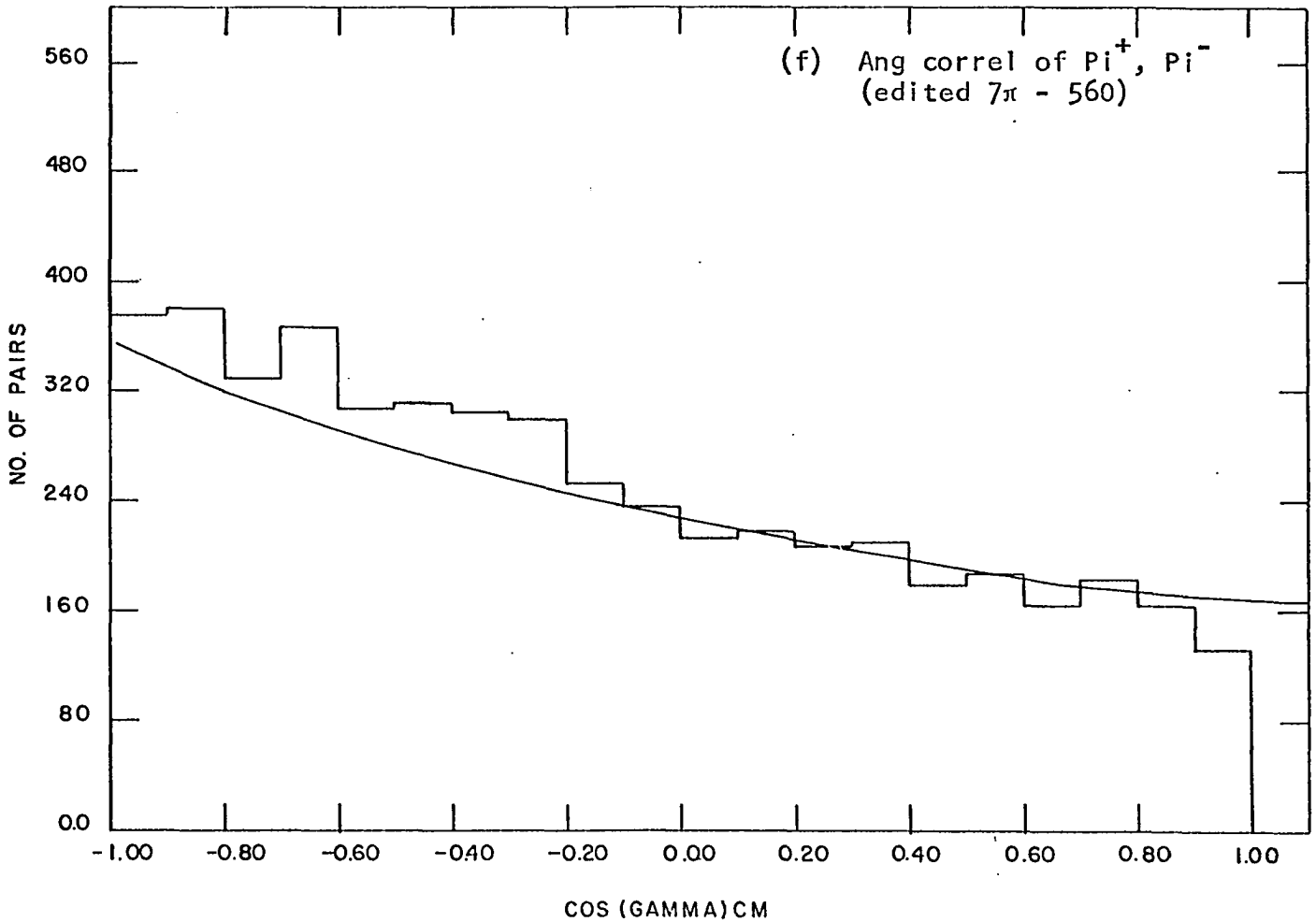

Figure 9f. Angular correlations in the center of mass system for pions from 7π samples

V. RESONANCE PRODUCTION

A. Known Resonances

All effective mass combinations for the two clearly identified samples of events, the 6π's and the 7π's, have been examined. The distributions of these combinations were compared with the distributions of Lorentz invariant phase space and, in every case, with the notable exceptions of the few treated below, showed remarkable agreement. This close agreement of the data with the predictions of phase space gave further, though by no means conclusive, assurance, that these samples neither included "fake" events in appreciable numbers nor excluded real events in a way that would bias the effective mass distributions.

In a search of the invariant mass plots for enhancements indicative of resonance activity, it must be kept in mind that with the six charged particles of these two final states, each event appears several times in any given distribution. This has the effect of "washing out" any structure that might be associated with a resonance since the ratio of background combinations to resonance structure is increased. In addition, there is a certain reluctance to give credence to apparent structure, because, with the large number of possible different effective mass combinations, there is an increased likelihood of finding a statistical fluctuation which appears significant.

The most prominent feature found in either of the final states is in the $\pi^+\pi^-$ effective mass plot from the 6π's. This plot is shown in Figure 10(a). The enhancement is immediately identifiable as the rho. To determine its mass and width as well as cross section, the data were

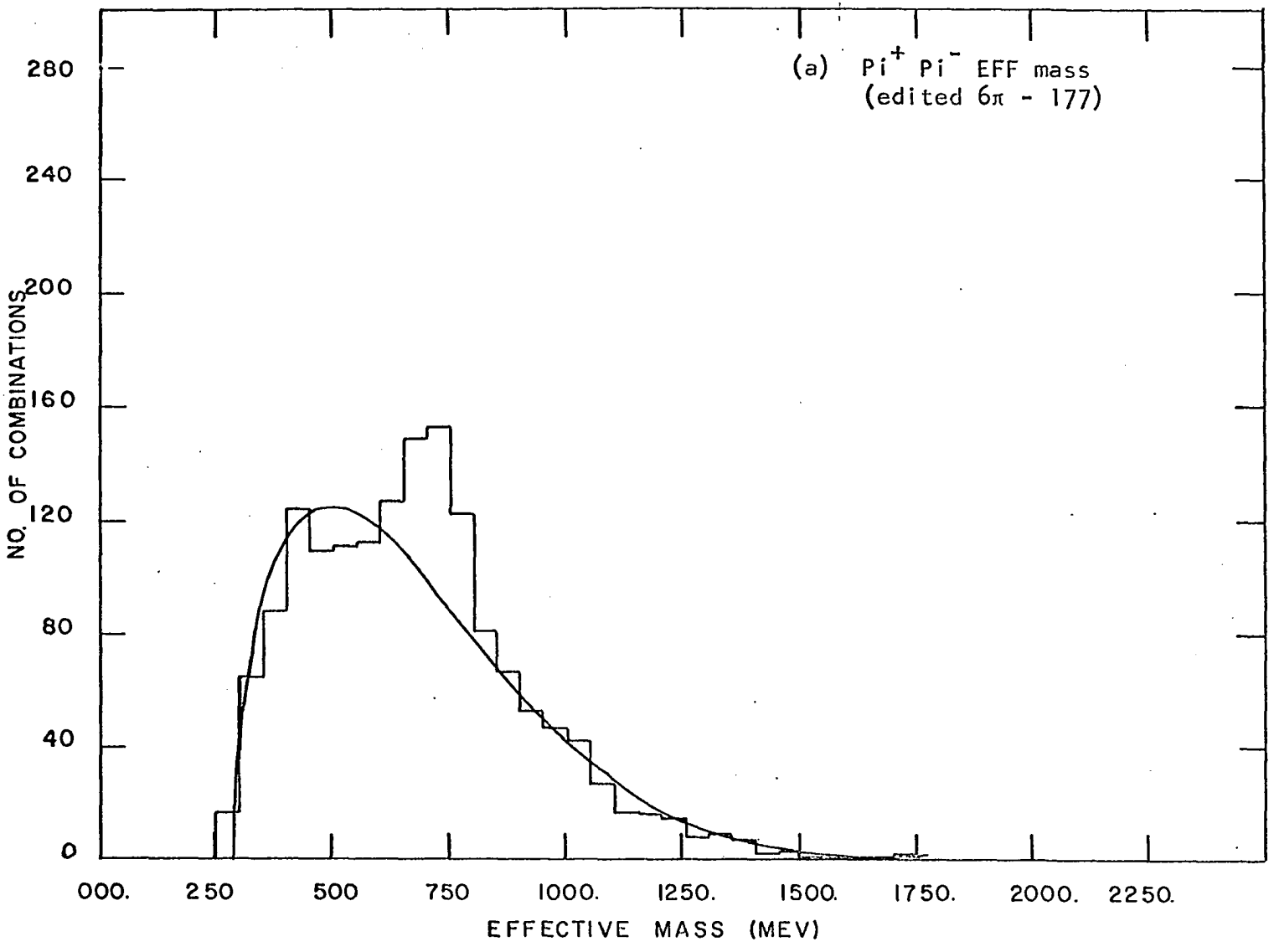

Figure 10a. Neutral two-body effective mass distribution of combinations with the mass value within the range 650 MeV and 820 MeV for events from 6π category

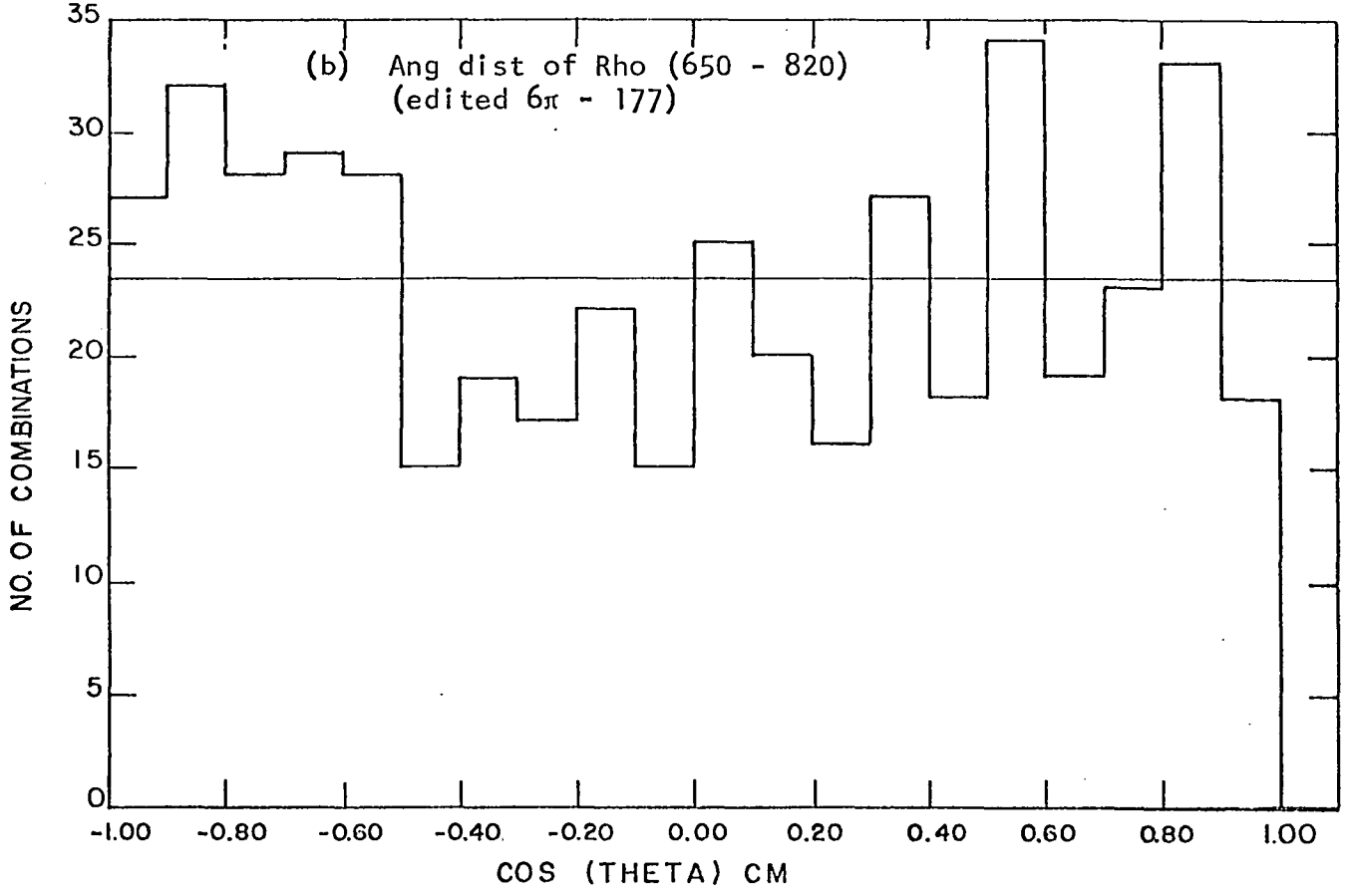

Figure 10b. Neutral two-body angular distribution of combinations with the mass value within the range 650 MeV and 820 MeV for events from 6π category.

fitted to an incoherent superposition of phase space and the Breit-Wigner curve (8). The mass and width producing the best fit, with their respective errors, are 734 ± 45 MeV and 146 ± 30 MeV. The best estimate of the central value is shifted, from the accepted mass of 760 MeV, but it is well known that, for a broad resonance, the energy dependence of the width causes a skewing of the resonance peak. Unfortunately this shift, as calculated from Jackson's formulas (8), accounts for only about nine MeV. In light of the uncertainty associated with the central value estimate, however, the discrepancy is probably not serious. Using the amount of phase space giving the best fit, as the amount of background, and using the same loss corrections as for the 6π's as a whole, the ρ^o cross section in the 6π's was estimated to be 1.00 ± 0.22 mb.

Finally, an examination of the $\bar{P}P$ center of mass angular distribution of the ρ with respect to the $\bar{P}$ produced the distribution in Figure 10(b). The forward-backward ratio is $+ 0.002 \pm 0.032$, consistent with a symmetric distribution.

Because of the substantial rho production in the 6π's and by inference from the four-prong events from this same experiment (9), ρ^o production is expected in the 7π sample. When the $\pi^+\pi^-$ effective mass distribution is examined, however, no significant enhancement in the region of the ρ^o is observed. Likewise, the $\pi^+\pi^o$ and $\pi^-\pi^o$ distributions from the 7π sample are phase space distributed, showing no sign of the $I_z = \pm 1$ states of the rho. Neutral rho production in the 7π final state is estimated at less than 7% and $\rho^+ + \rho^-$ production is estimated at less than 3%.

In addition to the rho, there are a number of other well established pion resonances, two of the most frequently observed being the ω^o and the

f^o. Though the neutral two pion effective mass distributions show no enhancement that might be interpreted as f^o production or other activity in either sample of events, the neutral three body combination in the 7π's shows a two standard deviation effect at the mass of the ω^o. Figure 11 gives the $\pi^+\pi^-\pi^o$ effective mass distribution for the 7π events.

Taking into account the diminutive size of this enhancement with respect to the background and the good agreement of the data with phase space over the remainder of the plot, it was felt that no serious fault could be found with fitting the distribution to an incoherent superposition of phase space and the Breit-Wigner curve. As a result of this fit, the mass and apparent width were found to be 790 ± 8 and 40 ± 10 and the degree of ω^o production as 23.2%, or 0.5 ± 0.27 mb.

B. Search for the 1670 MeV Meson State (G)

A CERN group (10) has observed an enhancement at 1670 MeV in the $\pi^+\pi^-$ system, but as has already been pointed out, this has no analogy in the present data. However, in the four-prong data from this experiment (9), a significant enhancement was reported at approximately 1640 ± 40 MeV in the neutral four pion effective mass distribution from the 5π sample. The width was given as 140 ± 40 MeV. Since the $I_z = \pm 1$ distributions showed no evidence of deviations from phase space at this energy it was interpreted to be an $I = 0$ effect. The observation of this enhancement in the four-prong data prompted an immediate search for a similar effect in the six-prong events. Figure 12 shows the $\pi^+\pi^-\pi^+\pi^-$ effective mass distributions from the 6π's and the 7π's. The phase space for the 7π plot has simply been normalized to the total number of events, but for the 6π

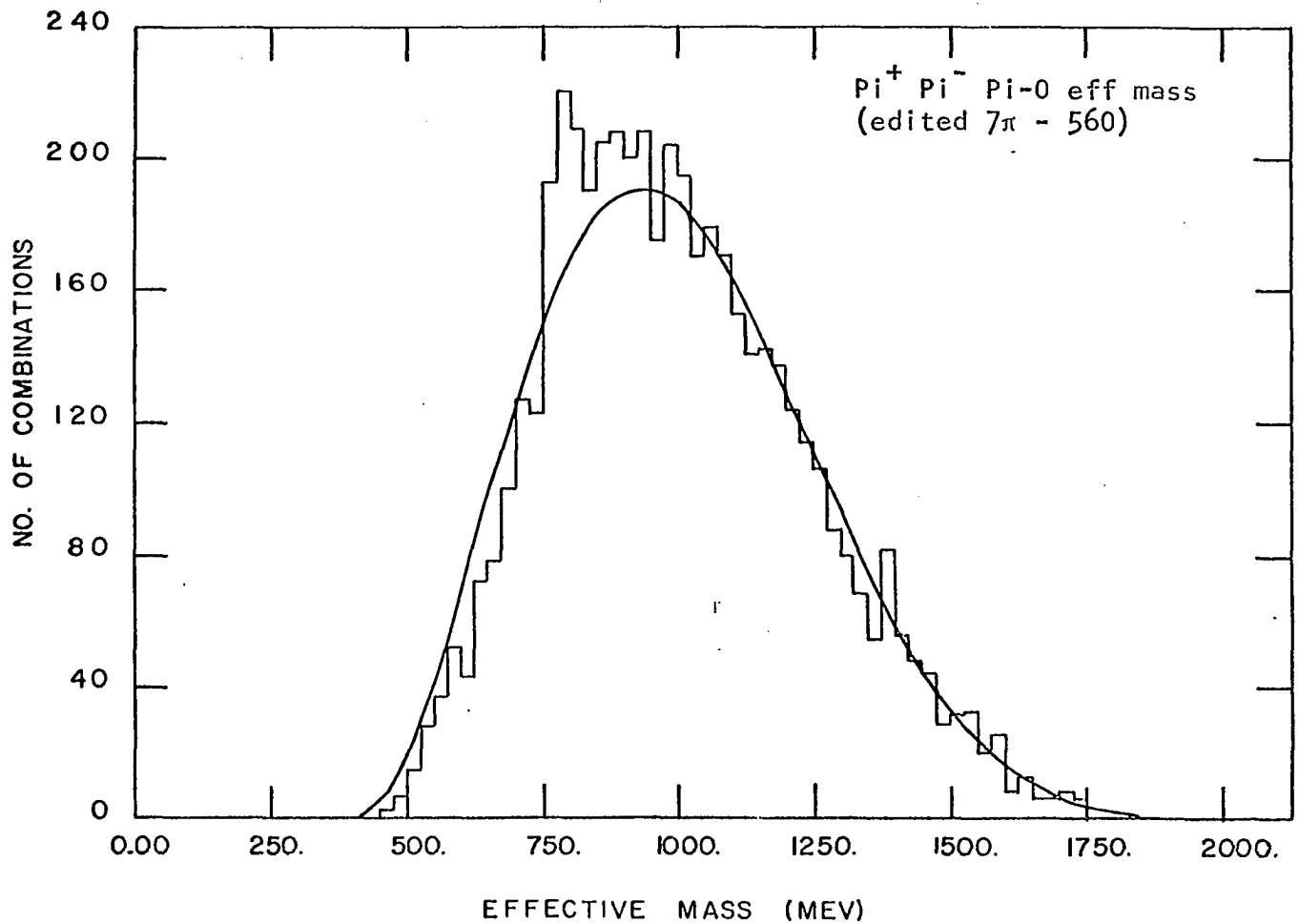

Figure 11. Neutral three-body effective mass distribution from pions of 7π sample

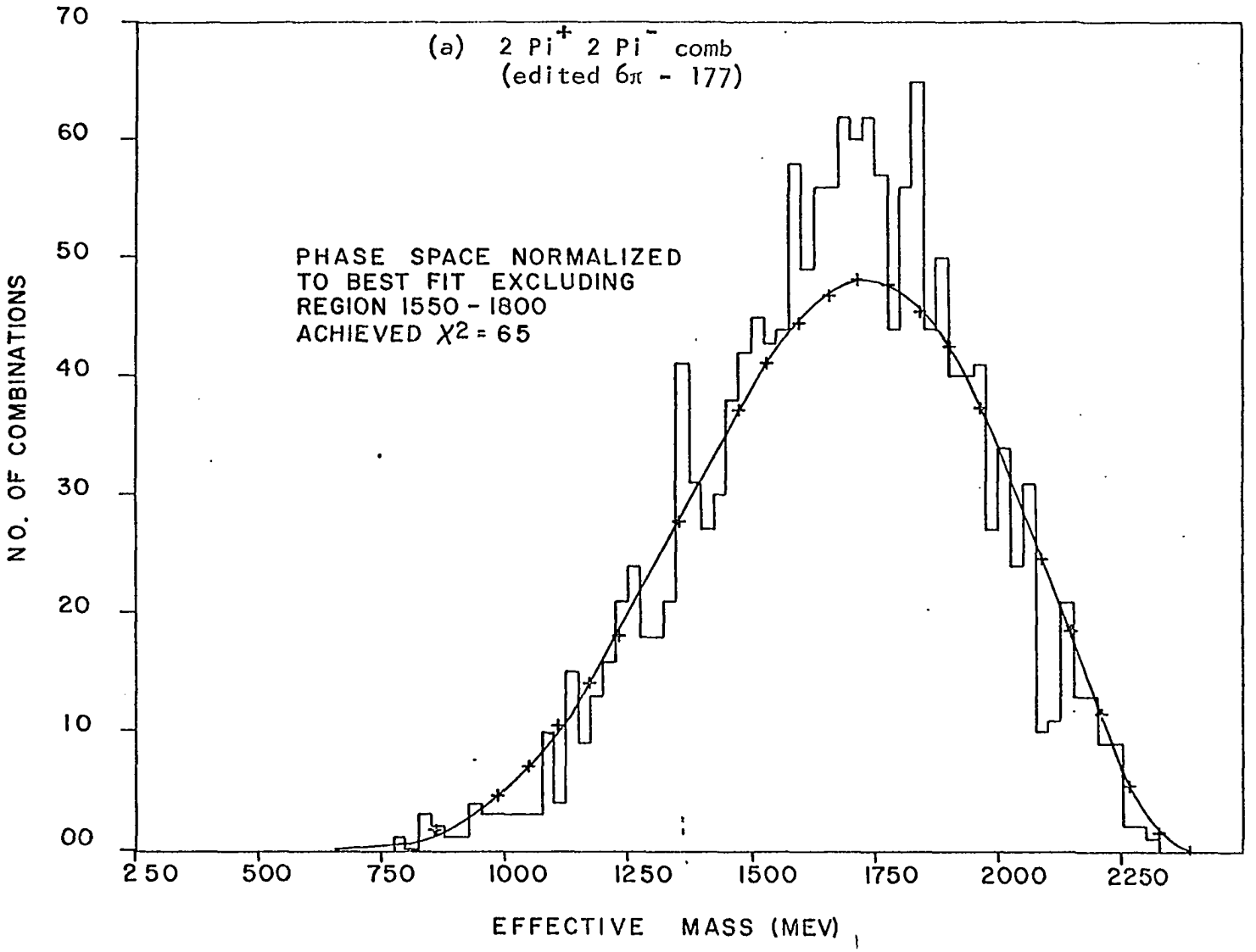

Figure 12a. Neutral four-body effective mass distribution from 6π events

distribution, the phase space was normalized to give the best fit to the data excluding the region 1550-1800 MeV. The 7π data show only an excellent agreement with phase space, but the 6π data do, indeed, seem to show an indication of structure close to the mass of the reported enhancement. To check the validity of this enhancement, the two doubly charged ($Q = \pm 2$) four pion effective mass distributions were combined and compared with the neutral four pion distribution. No similar build up of events in this region was observed in the check plot. To the same end, the 6π fits ambiguous with 7π's were examined for an unjustified collection of events in the region around 1650 MeV. No such accumulation was found.

It is important to realize that this enhancement must stand or fall on its own merits before any analogy can be drawn with the 5π effect (9). The experience gained from the examination of the 5π effect (9) is, of course, very useful here, but the 5π effect was part of a 2-body final state whereas a corresponding effect in the present data would be part of a 3-body final state making direct comparisons hazardous.

Because of the enhancements position at the peak of phase space and the structure close by, its significance is questionable. In an effort to reduce the background and also to test the enhancement itself, the data were tested in various ways. In the report of the 5π data (9), events taken from a slice between 1550 and 1800 were seen to peak strongly forward. To see if this property of the "resonance" to be produced in the forward direction might appear in the 6π data and help to reduce background, the center of mass angular distribution of combinations falling in and out of the 1550-1800 MeV mass range were compared. The distributions

showed no significant difference. Though the lack of a positive result eliminated this as a means of reducing the background, it did not necessarily imply that the enhancement seen in the 6π data could not be related to the effect in the 5π's. In the four-prong events the "resonance" was produced in the reaction

$$\bar{P} + P \rightarrow G + \pi^{o}$$

resulting in a two body final state. In the six-prongs, however, the reaction would have to be

$$\bar{P} + P \rightarrow G + \pi^{+} + \pi^{-} \quad ,$$

a three-body final state and the large combinatorial background could mask the forward production of the G. In addition, and probably more important, the production mechanisms for the G in the two final states would not necessarily have to be the same.

In a further attempt to reduce background, use was made of the fact that the G was observed to have a ρ - 2π decay mode (9). This time only the neutral four pion combinations which contained a two pion combination lying in the range 650-820 MeV were plotted. A small but noticeable increase in the signal to noise ratio was observed. A more effective way to use the observed ρ - 2π decay mode of the G in checking this enhancement is by examining the $\pi^{+}\pi^{-}$ effective mass distribution taken from $2\pi^{+} + 2\pi^{-}$ combinations with effective masses lying in different mass ranges. The percentages of excess ρ to the total numbers of $2\pi^{+} + 2\pi^{-}$ combinations were plotted against the effective mass. This plot is shown in Figure 13(a). Though the data do not permit a clear interpretation, ρ production seems

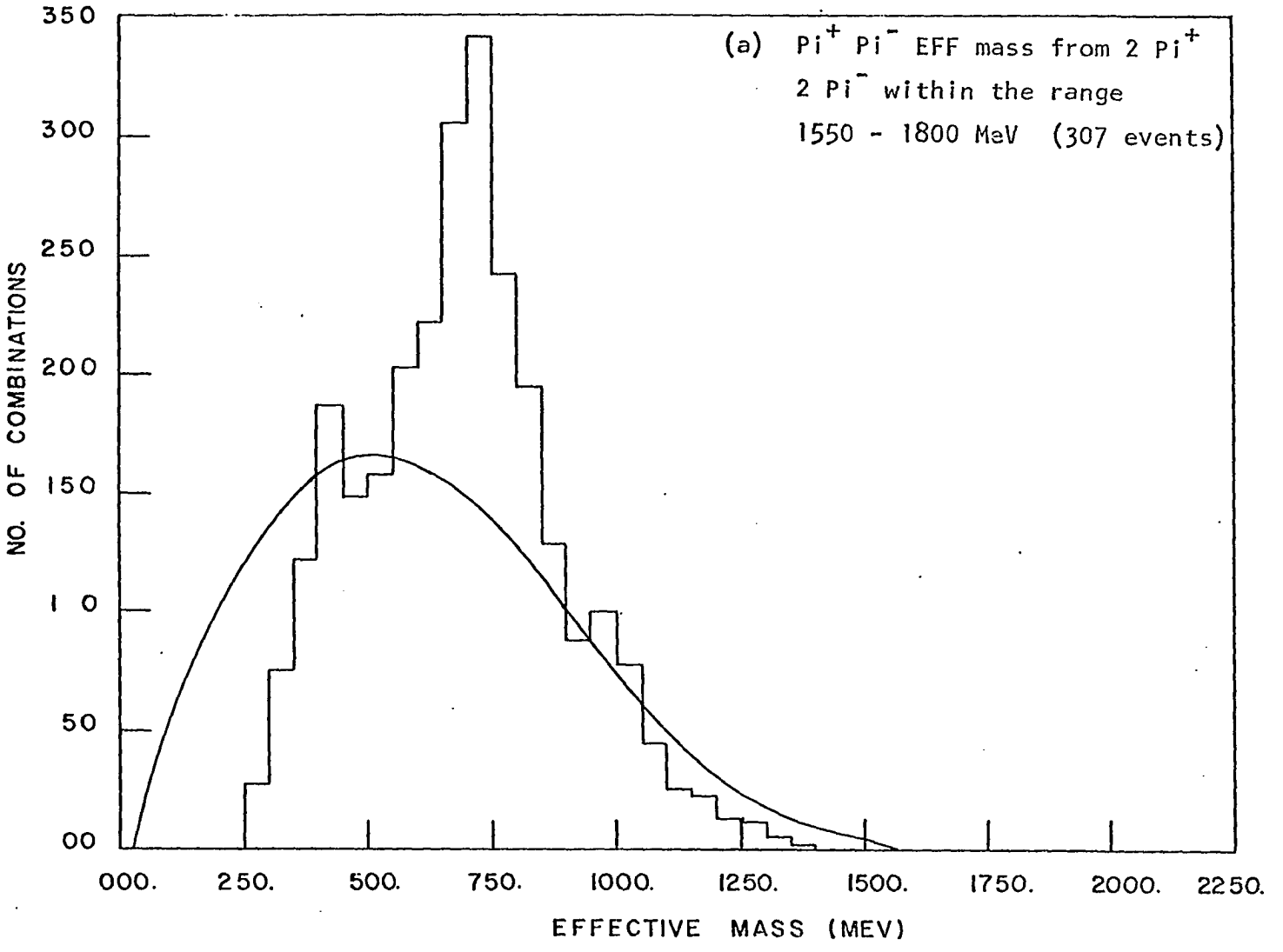

Figure 13a. Decay of the G meson into rho and two pions

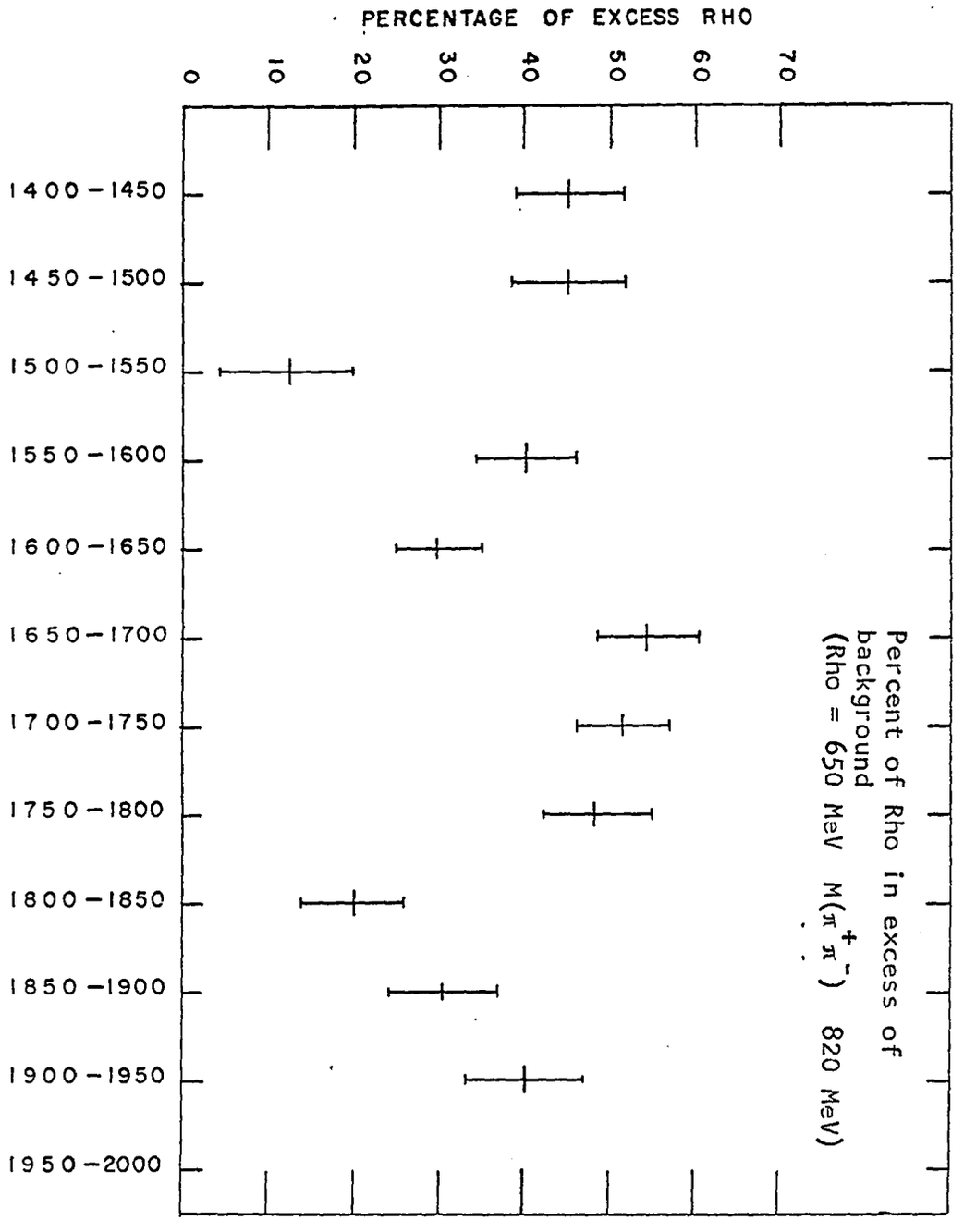

Figure 13b. Percent of rho in excess

enhanced in the region of the mass of the G.

Fitting the $2\pi^+ + 2\pi^-$ distribution to phase space plus Breit-Wigner yields the mass and the width of the enhancement as 1702 ± 50 MeV and 140 ± 40 MeV. These values are in better agreement with those of the CERN group (10) than with the results from the four-prong analysis of this experiment (9).

To estimate the branching ratio

$$R = \frac{(G \rightarrow \rho - 2\pi)}{(G \rightarrow 4\pi)}$$

the $\pi^+\pi^-$ effective mass distribution from the neutral four-body combinations lying between 1550 and 1800 was plotted. This distribution is shown in Figure 13(a). The amount of ρ coming from the G was assumed to be just that in excess of the amount contributed by a background found by extrapolating into the 1550-1800 region from the distributions made from the neutral four pion combinations on either side of the G region. By this method, the present data set the decay ratio at

$$R = 4.0 \pm 0.5 \ .$$

This is slightly greater than the result found in the four-prong events (9), but it is difficult to evaluate the difference, since the result varies considerably depending on how the background is estimated.

Though the enhancement seems quite prominent, and the production plot tends to support its validity, many of the 6π effective mass distributions have structure about the peak of phase space with nearly the same statistical validity. As a result, despite the evidence for this state, some serious doubts remain which will probably not be dispelled until additional data are available.

VI. BIBLIOGRAPHY

1. N. H. Xuong and G. R. Lynch, Phys. Rev. 128, 1849 (1962).

2. T. Ferbel, A. Firestone, J. Sandweiss, H. D. Taft, M. Gailloud T. W. Morris, W. J. Willis, A. H. Bachman, P. Baumel and R. M. Lea, Phys. Rev. 143, 1096 (1966).

3. G. Cocconi, Nuovo Cimento 33, 643 (1964).

4. Z. Koba and G. Takeda, Progr. Theoret. Phys., (Kyoto) 19, 269 (1958).

5. A. Stajano, Nuovo Cimento 28, 197 (1963).

6. K. Böckmann, B. Nellen, E. Paul, B. Wagini, I. Borecka, J. Diaz, U. Heeren, U. Liebermeister, E. Lohrmann, E. Raubold, P. Söding, S. Wolff, J. Kidd, L. Mandelli, L. Mosca, V. Pelosi, S. Ratti and L. Tallone, Elastic scattering, pion production and annihilation into pions in antiproton-proton interactions at 5.7 GeV/c, unpublished report, Bonn, Germany, Department of Physics, University of Bonn (1965).

7. G. Goldhaber, S. Goldhaber, W. Lee and A. Pais, Phys. Rev., 120, 300 (1960).

8. J. D. Jackson, Nuovo Cimento 34, 1644 (1964).

9. D. Lyon, Antiproton-Proton Annihilation into Four and Five Pions at 2.7 BeV/c, unpublished Ph.D. thesis, Ames, Iowa, Library, Iowa State University of Science and Technology, (1966).

10. M. Goldberg, F. Judd, G. Vegni, H. Winzeler, P. Fleury, J. Huc, R. Lestienne, G. De Rosny, R. Vanderhaghen, J. F. Allard, D. Drijard, J. Hennessy, R. Huson, J. Six, J. J. Veillet, A. Lloret, P. Musset, G. Bellini, M. Di Corato, E. Fiorini, P. Negri, M. Rollier, J. Crussard, J. Ginestet and A. H. Tran, Phys. Letters 17, 354 (1965).

VII. ACKNOWLEDGEMENTS

I would like to express my appreciation to Dr. William J. Kernan, Jr. for his patience and assistance and a great deal of valued counsel over the past three years.

My wife, Jackie, deserves special thanks for her help and encouragement, before and during the preparation of this dissertation.

The author would like to thank Dr. Lee S. Schroeder and Dr. Donald E. Lyon for helpful discussions at various times during this work and Dr. Lee S. Schroeder and Dr. Robert A. Leacock for their help in proofreading.

I am indebted to William J. Higby and the other members of the group's programming staff: Ann Nelson, Terry Schalk and Suzan Selby.

Deserving special thanks are Betty Pepper and her scanning staff: Jean Rostenbach, Joyce Tonne, Pat Tesdall, Marlene Frisk and Juanita Lincoln for many hours of hard work in the collection of data.

I am also grateful to Andrea Carlisle and Rita Wagstaff for their help in many capacities.

Finally, the author gratefully acknowledges the contribution of Brookhaven National Laboratory, especially the AGS and bubble chamber group personnel.